HEAT TRANSFER AND THERMAL RADIATION MODELLING

This is a briefing on thermal modelling of relevance to Spacecraft Thermal Control (STC). A more detailed analysis of Heat Transfer is presented aside.

HEAT TRANSFER AND THERMAL MODELLING

Thermal problems are mathematically stated as a set of restrictions that the sought solution must verify, some of them given explicitly as data in the statement, plus all the implicit assumed data and equations that constitute the expertise. It must be kept in mind that both, the implicit equations (algebraic, differential, or integral), and the explicit pertinent boundary conditions given in the statement, are subjected to uncertainties coming from the assumed geometry, assumed material properties, assumed external interactions, etc. In this respect, in modelling a physical problem, it is not true that numerical methods are just approximations to the exact differential equations; all models are approximations to real behaviour, and there is neither an exact model, nor an exact solution to a physical problem; one can just claim to be accurate enough to the envisaged purpose.

A science is a set of concepts and their relations. Good notation makes concepts more clear, and helps in the developments. Unfortunately, standard heat transfer notation is not universally followed, not only on symbols but in naming too; e.g. for thermo-optical properties, three different choices can be found in the literature:

A. Suffix *-ivity/-ance* may refer to intensive / extensive properties, as for resistivity / resistance.
B. Suffix *-ivity/-ance* may refer to own / environment-dependent properties; e.g. emissivity (own) / absorptance (depends on oncoming radiation). This is the choice followed here (and in ECSS-E-ST-31C-Thermal control).
C. Suffix *-ivity/-ance* may refer to theoretical / practical values; e.g. emissivity of pure aluminium / emittance of a given aluminium sample.

Thermal modelling approaches

A model (from Latin *modulus*, measure) is a representation of reality that retains its salient features. The first task is to identify the system under study. Modelling usually implies approximating the real

geometry to an ideal geometry (assuming perfect planar, cylindrical or spherical surfaces, or a set of points, a given interpolation function, and its domain), approximating material properties (constant values, isotropic values, reference material values, extrapolated values), and approximating the heat transfer equations (neglecting some contributions, linearising some terms, assuming a continuum media, assuming a discretization, etc.).

Modelling material properties introduces uncertainties because density, thermal conductivity, thermal capacity, emissivity, and so on, depend on the base materials, their impurity contents, bulk and surface treatments applied, actual temperatures, the effects of aging, etc. Most of the times, materials properties are modelled as uniform in space and constant in time for each material, but, the worthiness of this model and the right selection of the constant-property values, requires insight.

Heat transfer modes and the heat equation

Heat transfer is the relaxation process that tends to do away with temperature gradients in isolated systems (recall that within them $\nabla T \to 0$), but systems are often kept out of equilibrium by imposed boundary conditions. Heat transfer tends to change the local thermal state according to the energy balance, which for a closed system says that heat, Q (i.e. the flow of thermal energy from the surroundings into the system, driven by thermal non-equilibrium not related to work or the flow of matter), equals the increase in stored energy, ΔE, minus the flow of work inwards, W; which, for the typical case of a perfect incompressible substance (PIS, i.e. constant thermal capacity, c, and density, ρ) without energy dissipation ('non-dis'), it reduces to:

$$\text{What is heat? } (\equiv\text{heat flow}) \quad Q \equiv \Delta E - W = \Delta E + \int p\,\mathrm{d}V - W_{\text{dis}} = \Delta H - \int V\,\mathrm{d}p - W_{\text{dis}} = mc\Delta T|_{\text{PIS,non-dis}} \qquad (1)$$

Notice that heat implies a flow, and thus 'heat flow' is a redundancy (the same as for work flow). Further notice that heat always refers to heat transfer through an impermeable frontier, i.e. the former equation is only valid for closed systems, and that heat transfer refers to a unique interface area (the whole frontier, or part of it under the continuum approach) but it cannot be associated to energy transfer by radiation between two bodies, 1 and 2 (unless all the heat flowing through frontier-1 also flows through frontier-2).

The First Law applied to a regular interface (a non-dissipating one) implies that the heat loss by a system must pass integrally to another system, and the Second Law means that the hotter system gives off heat while the colder one takes it. In Thermodynamics, one refers sometimes to 'heat in an isothermal process', but this is a formal limit for small gradients and large periods. Here in Heat Transfer the interest is not in heat flow Q (named just heat, or heat quantity), but on heat-flow-rate $\dot{Q} = \mathrm{d}Q/\mathrm{d}t$ (named just heat rate, because the 'flow' characteristic is inherent to the concept of heat, contrary for instance to the concept of mass, to which two possible 'speeds' can be ascribed: mass rate of change, and mass flow rate). Heat rate, thence, is energy flow rate without work through an impermeable interface, or enthalpy flow rate at constant pressure without frictional work, i.e.:

$$\text{What is heat flux? (≡heat flow rate) } \dot{Q} \equiv \frac{dQ}{dt} = mc\frac{dT}{dt}\bigg|_{\text{PIS,non-dis}} \equiv KA\Delta T \qquad (2)$$

where the global heat transfer coefficient K (associated to a transfer area A and to the average temperature jump ΔT between the system and the surroundings), is defined by the former equation; the inverse of K is named global heat resistance coefficient $M \equiv 1/K$. Notice that this is the recommended nomenclature under the International System of Quantities (ISQ), with $G=KA$ being the global thermal transmittance and $R=1/G$ the global thermal resistance, although U has been used a lot in the literature instead of K, and R instead of M. Sometimes, heat flux refers to heat flow rate per unit area, $\dot{Q}/A$. instead of to $\dot{Q}$.

Notice that heat (related to a path integral in Thermodynamics) has the positive sign when it enters the system, but heat flux, related to a control area, cannot be ascribed a definite sign until we select one side.

In most heat-transfer problems, it is undesirable to ascribe a single average temperature to the system, and thus a local formulation must be used, defining the heat flow-rate density (or simply heat flux) as $\dot{q} \equiv \mathrm{d}\dot{Q}/\mathrm{d}A$. According to the corresponding physical transport phenomena, heat flux can be related to the local temperature gradient or to the temperature difference between the system wall (T_w) and the environment (far from the wall, T_∞, because at the wall local equilibrium implies $T=T_\mathrm{w}$). In the classical three distinct modes of heat transfer, namely: conduction, convection, and radiation; the following models are used:

$$\text{What is heat flux density (≈heat flux)? } \dot{q} = K\Delta T \begin{cases} \text{conduction} & \vec{\dot{q}} = -k\nabla T \\ \text{convection} & \dot{q} \equiv h\left(T_\mathrm{w} - T_\infty\right) \\ \text{radiation} & \dot{q} = \varepsilon\sigma\left(T_\mathrm{w}^4 - T_\infty^4\right) \end{cases} \qquad (3)$$

These three heat-flux models can also be viewed as: heat transfer within materials (conduction, Fourier's law), heat transfer at fluid-bathed walls (convection, Newton's law of cooling), and heat transfer through empty space (radiation, Stefan-Boltzmann's law of cooling for a body in a large environment). An important point to notice is the non-linear temperature-dependence of radiation heat transfer, what forces the use of absolute values for temperature in any equation with radiation effects. Conduction and convection problems are usually linear in temperature (if k and h are temperature-independent), that is why it is common practice to work in degrees Celsius instead of absolute temperatures when thermal radiation is not considered.

Thermal radiation is of paramount importance for heat transfer in spacecraft because the external vacuum makes conduction and convection to the environment non-existing, and it is analysed in detail below. For space applications, heat convection is only important within habitable modules, or in spacecraft incorporating heat-pipes or fluid-loops, for atmospheric flight during ascent or reentry, and for robots and habitats in the surface of Mars. The main difference with ground applications when concerning heat convection in space applications is the lack of natural convection under microgravity, although in all pressurised modules there is always a small forced air flow to help distribute oxygen and contaminants

(important not only to people but for fire detection and gas control). A small convective coefficient of h=(1..2) W/(m^2·K) is usually assumed for cabin air heating/cooling. Instead of the global convective coefficient, h, one might also use a local differential approach in the fluid side to compute heat convection at a wall, substituting $\dot{q} \equiv h\left(T_{\mathrm{w}} - T_{\infty}\right)$ by $\dot{q} = -k_f \nabla_n T$, where k_f is the thermal conductivity of the fluid an $\nabla_{\mathrm{n}} T$ the normal gradient at the wall of the fluid-temperature field, and solving the fluiddynamic problem by CFD.

Notice that, in the case of heat conduction, the continuum hypothesis has been introduced in (3), reducing the local formulation to a differential formulation to be solved in a continuum domain with appropriate boundary conditions (conductive to other media, convective to a fluid, or radiative to vacuum or other media), plus the initial conditions.

MODELLING THERMAL CONDUCTION

The famous heat equation (perhaps the most studied in theoretical physics) is the energy balance for heat conduction through an infinitesimal non-moving volume, which can be deduced from the energy balance applied to a system of finite volume, transforming the area-integral to the volume-integral with Gauss-Ostrogradski theorem of vector calculus, and considering an infinitesimal volume, i.e.:

$$\left.\frac{dH}{dt}\right|_p = \dot{Q} \quad \rightarrow \quad \int_V \rho c \frac{\partial T}{\partial t} dV = -\int_A \vec{q} \cdot \vec{n} dA + \int_V \phi dV \xrightarrow{V \to 0} \quad \rho c \frac{\partial T}{\partial t} = -\nabla \cdot \vec{q} + \phi = k \nabla^2 T + \phi \quad (4)$$

where ϕ has been introduced to account for a possible energy release rate per unit volume (e.g. by electrical dissipation, nuclear or chemical reactions), and constant conductivity is assumed for the last result, otherwise $-\nabla \cdot \vec{q} = -\nabla \cdot \left(-k \nabla T\right) = k \nabla^2 T + \nabla k \cdot \nabla T$. For steady-state conduction through a plate, temperature varies linearly within the solid, and the conduction term in (3) can be written as $\dot{q} = k\left(T_{\mathrm{w1}} - T_{\mathrm{w2}}\right)/L$, where L is the wall thickness.

As said above, in typical heat transfer problems, convection and radiation are only boundary conditions to conduction in solids, and not field equations; when a heat-transfer problem requires solving field variables in a moving fluid, it is studied under Fluid Mechanics' energy equation. In radiative problems like in spacecraft thermal control (STC), the local formulation is not usually pursued to differential elements but to small finite parts (lumps) which may be assumed to be at uniform temperature (the lumped network approach).

Thermal conductivities and other thermo-physical properties of materials

Generic thermo-physical properties of materials can be found in any Heat Transfer text (e.g. see Properties of solid materials), but several problems may arise, for instance:

- The composite material wanted is not in the generic list. Special applications like STC usually demand special materials with specific treatments that may introduce significant variations from common data (e.g. there are different carbon-carbon composites with thermal conduction in the range 400..1200 W/(m·K)).

- The surface treatment does not coincide with those listed. Particularly concerning the thermo-optical properties, uncertainties in solar absorptance (and to a lesser extent in emissivity) may be typically ±30% in metals and ±10% in non-metals, from generic data to actual surface state.
- The working temperature is different to the reference temperature applicable to the standard data value, and all material properties vary with temperature. For instance, very pure aluminium may reach k=237 W/(m·K) at 288 K, decreases to k=220 W/(m·K) at 800 K; going down, it is k=50 W/(m·K) at 100 K, increasing to a maximum of $k=25\cdot10^3$ W/(m·K) at 10 K and then decreasing towards zero proportionally to T, with $k=4\cdot10^3$ W/(m·K) at 1 K). Duralumin (4.4%Cu, 1%Mg, 0.75%Mn, 0.4%Si) has k=174 W/(m·K), increasing to k=188 W/(m·K) at 500 K.
- Thermal joint conductance between metals is heavily dependent on joint details difficult to characterise. And some joints are not fixed but rotating or sliding.

However dark the problem of finding appropriate thermal data may appear, the truth is that accuracy should not be pursued locally but globally, and that there are always uncertainties in the geometry, the imposed loads, and other interactions, which render the isolated high precision quest useless and thus wasteful.

Unless experimentally measured on a sample, thermal conductivities from generic materials may have uncertainties of some 10%. Most metals in practice are really alloys, and thermal conductivities of alloys are usually much lower than those of their constituents, as shown in Table 1; it is good to keep in mind that conductivities for pure iron, mild steel, and stainless steel, are (80, 50, 15) W/(m·K), respectively. Besides, many common materials like graphite, wood, holed bricks, reinforced concrete, and modern composite materials, are highly anisotropic, with directional heat conductivities. And measuring k is not simple at all: in fluids, avoiding convection is difficult; in metals, minimising thermal-contact resistance is difficult; in insulators, minimising heat losses relative to the small heat flows implied is difficult; the most accurate procedures to find k are based on measuring thermal diffusivity $a=k/(\rho c)$ in transient experiments.

Table 1. Thermal conductivities of some alloys and its elements.

Alloy	k [W/(m·K)] of alloy	k [W/(m·K)] of base element	k [W/(m·K)] of other elements
Mild steel G-10400 (99% Fe, 0.4% C)	51 (at 15 ºC) 25 (at 800 ºC)	80 (Fe)	2000 (C, diamond) 2000 (C, graphite, parallel) 6 (C, graphite, perpendicular) 2 (C, graphite amorphous)
Stainless steel S-30400 (18..20% Cr, 8..10% Ni)	16 (at 15 ºC) 21 (at 500 ºC)	80 (Fe)	66 (Cr) 90 (Ni)

Unless experimentally measured on the spot, solar absorptance, α, and infrared emissivity, ε, of a given surface can have great uncertainties, which in the case of metallic surfaces may be double or half, due to minute changes in surface finishing and weathering.

Thermal inertia and energy storage

A basic question on thermal control systems is to know how long the heating or cooling process takes (i.e. the thermal inertia of the system), usually with the intention to modify it, either to make the system more permeable to heat, more insulating, or more 'capacitive', to retard a periodic cooling/heating wave.

When the heat flow can be imposed, the minimum time required is obtained from the energy balance, $\mathrm{d}H/\mathrm{d}t=\dot{Q}$, yielding $\Delta t=mc\Delta T/\dot{Q}$.

When a temperature gradient is imposed, an order-of-magnitude analysis of the energy balance, $\mathrm{d}H/\mathrm{d}t=\dot{Q}\ \rightarrow\ mc\Delta T/\Delta t=KA\Delta T$, shows that the relaxation time is of the order $\Delta t=mc/(KA)$, and, depending on the dominant heat-transfer mode in K, several extreme cases can be considered:

- Conduction driven case. The time it takes for the body centre to reached a mid-temperature, representative of the forcing step imposed at the surface, is $\Delta t=L^2/a$, i.e. increases with the square of the size, decreases with thermal diffusivity, and is independent of temperature.
- Convection driven case. In this case, $\Delta t=\rho cL/h$.
- Radiation driven case. In this case, $\Delta t=\rho cL/h$, with h being the net thermal radiation flux; if irradiance E is dominant (e.g. solar gain with E=1370 W/m^2), then $h=E$; if exitance M is dominant and there are only losses to the deep-space background at T_0=2.7 K (≈0), then $h=\varepsilon\sigma T^3$; in the case of heat radiation exchange with a blackbody at T_0, then $h=\varepsilon\sigma(T^2+T_0^2)(T+T_0)$.

When thermal loads are transient, with short pulses, the best way to protect equipment from large temperature excursions is to increase the thermal inertia of the system, preferably by adding some phase change material like a salt or an organic compound (within a closed container with good conductive characteristics).

Exercise 1. Find the time it takes for the centre of a 1 cm glass sphere to reach a representative temperature in a heating or cooling process.

Sol.: The time it takes for the centre to reach a representative temperature in a heating or cooling process (e.g. a mid-temperature between the initial and the final), is $\Delta t=\rho cL^2/k$=2500·800·(0.01/6)^2/1=6 s, where the characteristic length of a spherical object, $L=V/A=(\pi D^3/6)/(\pi D^2)=D/6$, has been used.

Numerical discretization. Nodal elements

Numerical solutions are the rule in solving practical heat transfer problems because analytical formulation can only be found for very simple geometries and boundary conditions. Numerical methods transform the continuous problem into a discrete problem, thus, instead of yielding a continuous solution valid at every point in the system and every instant in time, and every value of the parameters, numerical methods only yield discrete solutions, valid only at discrete points in the system, at discrete time intervals, and for discrete values of the parameters. However gloom the numerical approach may sound, it has two crucial advantages:

- Can provide a solution to any practical problem, however complicated it may be (not just steady one-dimensional, constant-property ideal models). In any case, it is most important to realise that

any practical problem is at the end an intermediate idealisation aiming at practical answers (e.g. nobody takes account of the infinite figures in π; 3 may be a good-enough approximation, and 3.1416 already an accuracy illusion).

- The discretization can be refined as much as wanted (of course, at the expense in computing time and memory, and operator's burden). In any case, it is wise to start with as few unknowns as feasible, for an efficient feedback (most of the first trials suffer from infancy problems that are independent on the finesse of the discretisation). Any practitioner knows that refinements should follow coarse work, and not the contrary.

Most commercial packages are based on the finite element model (FEM). However, to gain insight in heat transfer, once the few analytical solutions are mastered, it is preferable to do numerical simulations in simple heat transfer problems, using the finite difference method (FDM), due to its simplicity (simple 1D or 2D transient problems only demand a few lines of code); the penalty is that FDM demands a simple geometry with a structured grid, i.e. FDM becomes complicated in systems with non-rectangular (or non-cylindrical, or non-spherical) geometries.

FDM starts by establishing a mesh of nodes in the domain, i.e. a set of points in space where the function (temperature) is to be computed. There should be a node where the function is sought; at least one node at each boundary or singularity (the most important locations, and were boundary conditions are imposed), plus a few others for better resolution (say between 10 and 50). Thermal conductivities between nodes are averaged as explained below, and thermal capacities are assigned to each node to solve the transients. Spatial gradients are best discretised by centred differences, and time discretization is simplest if using advance differences, namely:

$$\frac{dT}{dx} \to \frac{T_{i+1}^{j} - T_{i-1}^{j}}{2\Delta x} \quad \text{and} \quad \frac{d^2T}{dx^2} \to \frac{T_{i+1}^{j} - T_{i}^{j} + T_{i-1}^{j}}{(\Delta x)^2}$$
$$\frac{dT}{dt} \to \frac{T_{i}^{j+1} - T_{i}^{j}}{\Delta t} \qquad (5)$$

With this explicit scheme, the time step must be limited to avoid numerical instability. The stability criterion can be explained in terms of the Second Law of Thermodynamics: if we imagine the thermal relaxation of a node at T_1 with the surroundings nodes at $T_0<T_1$ (2 in one-dimensional problems); the discretized heat equation can be written as $\Delta_t T/\Delta t=2a\Delta_x T/(\Delta x)^2$, but the Second Law forbids the temporal variation $\Delta_t T$ to surpass the spatial variation $\Delta_x T$, i.e. $\Delta_t T <\Delta_x T$, implying $2a\Delta t/(\Delta x)^2<1$ or $Fo<1/2$ ($Fo<1/4$ for 2D, $Fo<1/6$ for 3D).

An explicit scheme for 1D planar conduction, valid for walls, rods, bars, layers, and so on, with possible variation of properties and heat-path cross-section, and possible volumetric sources and lateral loses, is:

$$\rho_i A_i \Delta x\, c_i \frac{T_i^{j+1}-T_i^j}{\Delta t} = k_{i+}A_{i+}\frac{T_{i+1}^j-T_i^j}{\Delta x} - k_{i-}A_{i-}\frac{T_i^j-T_{i-1}^j}{\Delta x} + \phi_i^j A_i \Delta x - p_i \Delta x\left[h_i\left(T_i^j - T_\infty\right) + \varepsilon_i\sigma\left(T_i^4 - T_\infty^4\right) - E_i\right]$$

$$\rightarrow T_i^{j+1} = T_i^j + \frac{\Delta t}{\rho_i c_i A_i}\left[k_{i+}A_{i+}\frac{T_{i+1}^j-T_i^j}{(\Delta x)^2} - k_{i-}A_{i-}\frac{T_i^j-T_{i-1}^j}{(\Delta x)^2} + \phi_i^j A_i - p_i\left[h_i\left(T_i^j - T_\infty\right) + \varepsilon_i\sigma\left(T_i^4 - T_\infty^4\right) - E_i\right]\right] \quad (6)$$

where space and time are discretized in constant steps ($j\Delta t$ and $i\Delta x$, respectively), $T_i^j = T(j\Delta t, i\Delta x)$, ρ_i and c_i are the density and thermal capacity at stage i, A_i the cross-section area, k_{i+} and k_{i-} the thermal conductivity averaged to each side (i.e. $k_{i+}=(k_{i+1}+k_i)/2$ and $k_{i-}=(k_{i-1}+k_i)/2$), ϕ_i a volumetric hear source, pi the perimeter for lateral heat loses (e.g. $p=\pi D$ in a rod of diameter D; mind that a plate of width w may be exposed by both sides, $p=2w$, or just by one), h_i the lateral convective coefficient towards a fluid at T_∞, ε_i the emissivity for infrared radiation, and E_i a possible irradiation gain [W/m^2]. In the case of constant properties, (6) reduces to:

$$T_i^+ = T_i + Fo\left(T_{i+} - 2T_i + T_{i-}\right) + \frac{\phi\Delta t}{\rho c} - \frac{p\Delta t}{\rho c A}\left[h\left(T_i^j - T_\infty\right) + \varepsilon\sigma\left(T_i^4 - T_\infty^4\right) - E\right] \quad (7)$$

where $Fo=k\Delta t/(\rho c\Delta x^2)$ is the Fourier number. It is convenient to place nodal points at the ends, i.e. to choose $i=1$ at $x=0$ and $i=N+1$ at $x=L_x$, in spite of the fact that then the end elements only extend $\Delta x/2$. As for the two boundary conditions, the case of constant end temperature is trivial, $T_1^{j+1} = T_1^j$ =constant and/or $T_{N+1}^{j+1} = T_{N+1}^j$, but the case of adiabatic end, $\dot{Q}_0 = -kA\left(T_2^j - T_2^j\right)\big/\Delta x = 0$, is more delicate (we cannot impose $T_1^{j+1} = T_2^{j+1}$ in an explicit scheme);

$$T_1^+ = T_1 + 2Fo\left(T_2 - T_1\right) + \frac{\Delta t}{\rho c A}\left[\frac{\dot{Q}_0}{2\Delta x} + \phi A - ph\left(T_1 - T_\infty\right)\right] \overset{\dot{Q}_0=0}{=} 2FoT_2 + \left(1-2Fo\right)T_1 + \frac{\Delta t}{\rho c A}[\ ] \overset{Fo=\frac{1}{2}}{\approx} T_2 \quad (8)$$

i.e. with $Fo\approx 1/2$ and a small Δt, for adiabatic ends we can impose $T_1^{j+1} = T_2^j$ and/or $T_{N+1}^{j+1} = T_N^j$. More involved boundary conditions, perhaps with prescribed heat flows, $\dot{Q}_0 \neq 0$, can be worked out with (7).

Thermal conduction averaging

There are many multidimensional thermal conduction configurations which can be approximated by an equivalent one-dimensional model, greatly simplifying the analysis. The most common case is approximate a compound plate (e.g. a printed circuit board, PCB, made of copper lines to transmit power and data, and of electrically-insulating material, including the small electronic devices soldered to the PCB), to a uniform planar rectangular plate. Besides this multilayer-plate case, we present the thickness-varying case, and the honeycomb case.

Multilayer plate

Consider a plate made of n layers ($i=1..n$), each one with thickness δ_i and area-fraction coverage f_i (interconnected, and with the remaining $1-f_i$ covered by non-conducting media), as sketched in Fig. 1a for a PCB; in this sketch there is a continuous bottom layer made of copper (used as heat sink), a thicker layer of electrical insulator made of fibre-reinforced epoxy (FR4), which constitutes the PCB structural element, a top layer partially covered with copper lines connecting the components, and a solder mask (a

thin polymer protecting the copper lines, since untreated copper oxidizes quickly) were openings for connections are made by photolithography.

If the two ends along the plane (x-direction) are kept steady with a temperature difference ΔT_x, the heat conducted is the sum of heat conducted through each layer, i.e. $\dot{Q}_x = \sum\left(k_i A_i\right)\left(\Delta T_x / L_x\right)$, where k_i and A_i are the thermal conductivity and cross-section area of the i-layer, which, if constituted by a main conducting material, can be substituted by its conductivity, k_i, and the effective cross-section area, $A_i=f_i\delta_i L_z$, where f_i is the average cross-section area occupied by the main conductor δ_i is the i-layer thickness in the y-direction ($\Sigma\delta_i=\delta_y$), and L_z the plate length in the third dimension. Hence, an effective thermal conductivity, k_{eff}, can be defined for approximating the real multilayer plate by a uniform plate:

$$\dot{Q}_x = k_{\text{eff},x}\delta_y L_z \frac{\Delta T_x}{L_x} = \sum_{\text{layers}}\left(k_i f_i \delta_i\right) L_z \frac{\Delta T_x}{L_x} \quad \rightarrow \quad k_{\text{eff},x} = \frac{\sum_{\text{layers}} k_i f_i \delta_i}{\delta_y} \tag{9}$$

On the other hand, if we want to average transversally instead of along the plate, the total heat flow is the combination in a series of layers, i.e. the compound wall solution:

$$\dot{Q}_y = k_{\text{eff},y} L_x L_z \frac{\Delta T_y}{\delta_y} = \frac{\Delta T_x}{\sum_{\text{layers}} \frac{\delta_i}{k_i f_i L_x L_z}} \quad \rightarrow \quad k_{\text{eff},y} = \frac{\delta_y}{\sum_{\text{layers}} \frac{\delta_i}{k_i f_i}} \tag{10}$$

As for thermal inertia, mc, the effective thermal capacity to be applied is $c_{\text{eff}}=\Sigma m_i c_i / m$.

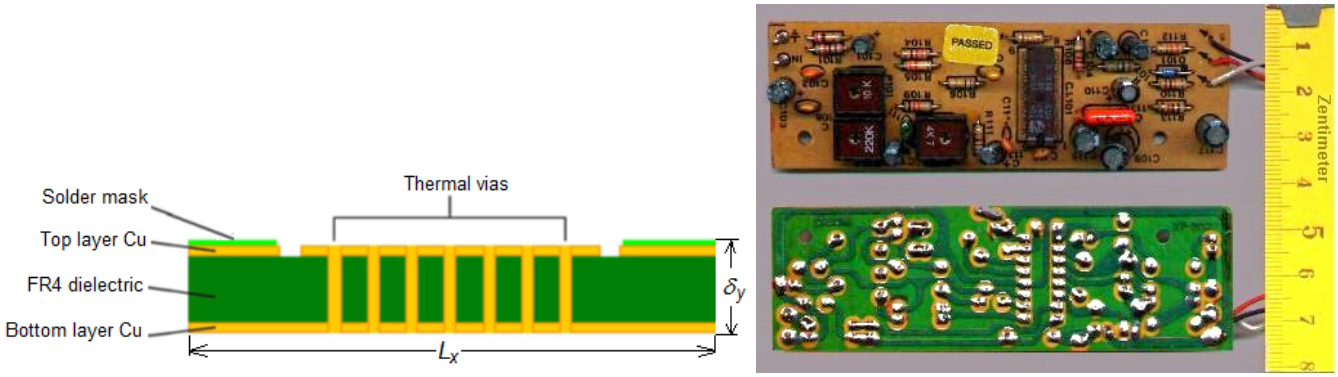

Fig. 1. a) Cross-section sketch of a PCB (about 1 mm thick). b) Example pictures of component-side and solder-side in a PCB.

Exercise 2. Find the in-plane effective thermal conductivity, and the normal thermal resistance for a component covering a 37.5×37.5 mm^2 area, in a PCB of 150×100×1.5 mm^3, made of a single FR-4 layer, with a top copper layer of 70 μm with 20% of metal, and a bottom copper layer of 70 μm with 100% of metal.

Sol.: PCB one-side area $A_{\text{PCB}}=150\times100=15\cdot10^{-3}$ m^2; main-component area $A_{\text{comp}}=37.5\times37.5=1.4\cdot10^{-3}$ m^2. As copper only covers 20% of the top layer (the other 80% can be neglected for thermal conduction), applying (9) and (10) with k_{FR4}=0.25 W/(m·K) across, k_{FR4}=0.5 W/(m·K) along, and k_{Cu}=400 W/(m·K), we get:

-along the card:

$$k_{\text{eff,along}} = \sum_{\text{layers}} \frac{k_i f_i \delta_i}{\delta_{\text{PCB}}} = \frac{k_{\text{Cu,1}} f_{\text{Cu,1}} \delta_{\text{Cu,1}} + k_{\text{FR4along}} f_{\text{FR4}} \delta_{\text{FR4}} + k_{\text{Cu,2}} f_{\text{Cu,2}} \delta_{\text{Cu,2}}}{\delta_{\text{PCB}}} =$$

$$= \frac{400 \cdot 0.2 \cdot 0.07 \cdot 10^{-3} + 0.5 \cdot 1 \cdot (1.5 - 2 \cdot 0.07) \cdot 10^{-3} + 400 \cdot 1 \cdot 0.07 \cdot 10^{-3}}{1.5 \cdot 10^{-3}} = 23 \frac{\text{W}}{\text{m} \cdot \text{K}}$$

-normal to the card:

$$R = \frac{\delta_{\text{comp}}}{k_{\text{eff,n}} A_{\text{comp}}} = \sum_{\text{layers}} \frac{\delta_i}{k_i f_i A_{\text{comp}}} = \frac{0.07 \cdot 10^{-3}}{400 \cdot 0.2 \cdot (1.4 \cdot 10^{-3})} + \frac{1.36 \cdot 10^{-3}}{0.25 \cdot 1 \cdot (1.4 \cdot 10^{-3})} + \frac{0.07 \cdot 10^{-3}}{400 \cdot 1 \cdot (15.4 \cdot 10^{-3})} = 3.9 \frac{\text{K}}{\text{W}}$$

The effective conductivity across the board under the component (assuming the same copper factor, is:

$$k_{\text{eff,}yacross} = \frac{\delta_z}{\sum_{\text{layers}} \frac{\delta_i}{k_i f_i}} = \frac{\delta_{PCB}}{\frac{\delta_{\text{Cu,1}}}{k_{\text{Cu,1}} f_{\text{Cu,1}}} + \frac{\delta_{\text{FR4}}}{k_{\text{FR4}\perp}} + \frac{\delta_{\text{Cu,2}}}{k_{\text{Cu,2}}}} = \frac{1.5 \cdot 10^{-3}}{\frac{0.07 \cdot 10^{-3}}{400 \cdot 0.2} + \frac{1.5 \cdot 10^{-3}}{0.25} + \frac{0.07 \cdot 10^{-3}}{400}} = 0.28 \frac{\text{W}}{\text{m} \cdot \text{K}}$$

Non-uniform thickness

Consider a plate made of a single material but of non-uniform thickness (e.g. a plate ribbed or pocketed to strengthen it while minimising mass). To make the explanation simpler, let we think of a two-dimensional case with thickness profile varying only along the x-coordinate, $\delta(x)$; the equivalent thickness, δ_e, of a uniform plate is found by imposing mass conservation: $\delta_e = \int \delta(x) \mathrm{d}x / L_x$. The equivalent thermal conductivity must be found from Fourier's law:

$$\dot{Q}_x = k_{\text{eff},x} \delta_e L_z \frac{\Delta T_x}{L_x} = k \delta(x) L_z \frac{\mathrm{d}T_x}{\mathrm{d}x} = \frac{\Delta T_x}{\int_0^{L_x} \frac{\mathrm{d}x}{k \delta(x) L_z}} \quad \rightarrow \quad k_{\text{eff},x} = k \frac{L_x}{\delta_e \int_0^{L_x} \frac{\mathrm{d}x}{\delta(x)}} \qquad (11)$$

Another way out is to find the effective thickness for the nominal thermal conductivity:

$$\dot{Q}_x = k \delta_{\text{eff}} L_z \frac{\Delta T_x}{L_x} = k \delta(x) L_z \frac{\mathrm{d}T_x}{\mathrm{d}x} = k L_z \frac{\Delta T_x}{\int_0^{L_x} \frac{\mathrm{d}x}{\delta(x)}} \quad \rightarrow \quad \delta_{\text{eff}} = \frac{L_x}{\int_0^{L_x} \frac{\mathrm{d}x}{\delta(x)}} \qquad (12)$$

Exercise 3. Find the effective thermal conductivity and the effective thickness of the ribbed aluminium (A-7075) plate sketched in Fig. E3, machined from a 500×500×5 mm^3 uniform plate, with six equi-spaced parallel grooves 60 mm wide and 3 mm deep were milled, leaving 7 equi-spaced ribs 20 mm wide.

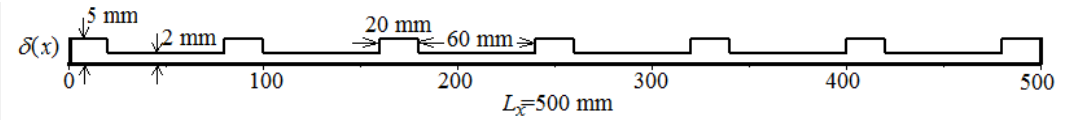

Fig. E3. Cross-section of the ribbed plate.

Sol.: From mass conservation, the averaged thickness is $\delta_{\text{mean}}=\int\delta(x)\mathrm{d}x/L_x=2.84$ mm (closer to the minimum thickness of 2 mm, than to the maximum of 5 mm, since the 2 mm spans are wider than the 5 mm ones). The effective thermal conductivity for that mean thickness is obtained from (11) with k=134 W/(m·K) for A-7075:

$$k_{\text{eff}} = k\frac{L_x}{\delta_{\text{mean}}\int_0^{L_x}\frac{\mathrm{d}x}{\delta(x)}} = 134\frac{0.5}{\left(2.84\cdot10^{-3}\right)\cdot208} = 113\ \frac{\text{W}}{\text{m}\cdot\text{K}}$$

i.e. the effective thermal conductivity to be used in the equivalent uniform-thickness plate is 15% lower than the nominal one. Conversely, if we want to find the effective thickness to be used with the nominal k=134 W/(m·K) for A-7075, we use (12) and get:

$$\delta_{\text{eff}} = \frac{L_x}{\int_0^{L_x}\frac{\mathrm{d}x}{\delta(x)}} = \frac{0.5}{208} = 2.40\ \text{mm}$$

The heat transfer along the plate can be computed from $\dot{Q}=kA\Delta T/L_x=k_{\text{eff}}\delta_{\text{mean}}L_z\,\Delta T/L_x=k\delta_{\text{eff}}L_z\,\Delta T/L_x$, where $k_{\text{eff}}\delta_{\text{mean}}=k\delta_{\text{eff}}$ (113·2.84= 134·2.40).

Honeycomb panels

Honeycomb panels (Fig. 2) are structural elements with great stiffness-to-mass ratio, widely used in aerospace vehicles. Heat transfer through honeycomb panels is non-isotropic and difficult to predict. If the effect of the cover faces is taken aside, and convection and radiation within the honeycomb cells can be neglected in comparison with conduction along the ribbons (what is the actual case in aluminium-honeycombs), heat transfer across each of the dimensions is:

$$\left.\begin{aligned}
\dot{Q}_x &= kF_xA_x\frac{\Delta T_x}{L_x} \quad \text{with} \quad F_x=\frac{3}{2}\frac{\delta}{s}\\
\dot{Q}_y &= kF_yA_y\frac{\Delta T_y}{L_y} \quad \text{with} \quad F_y=\frac{\delta}{s}\\
\dot{Q}_z &= kF_zA_z\frac{\Delta T_z}{L_z} \quad \text{with} \quad F_z=\frac{8}{3}\frac{\delta}{s}
\end{aligned}\right\} \qquad (13)$$

where F is the factor modifying solid body conduction (the effective conductive area divided by the plate cross-section area), which is proportional to ribbon thickness, δ, divided by cell size, s (distance between opposite sides in the hexagonal cell, not hexagon side, a, in Fig. 2; $s=\sqrt{3}\,a$), and depends on the

direction considered: x is along the ribbons (which are glued side by side), y is perpendicular to the sides, and z is perpendicular to the panel. For instance, for the rectangular unit cell pointed out in Fig. 2, of cross-section area $3as$, the solid area is $8a\delta$, and the quotient is $F_z=(8/3)\delta/s$.

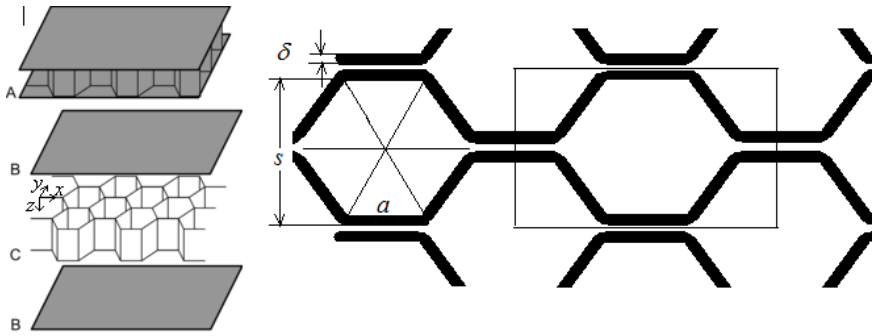

Fig. 2. Structure of a honeycomb sandwich panel: assembled view (A), and exploded view (with the two face sheets B, and the honeycomb core C) (Wiki). Ribbons run along the x direction, and are glued side by side in counter-phase along the y direction as detailed.

Mean density scales with F_z (e.g. for a core made of aluminium foil (ρ=2700 kg/m^3, k=150 W/(m·K)) of thickness δ=30 μm in s=3 mm cell pattern, $F_z=(8/3)(\delta/s)=(8/3)(0.03/3)=0.027$, and the mean core-panel values are $\rho=2700\cdot0.027=73$ kg/m^3, and $k=150\cdot0.027=4$ W/(m·K).

Example 1. Satellite platform with embedded battery modules.
Example 2. Thermal transients in a CFRP wall.
Example 3. Printed circuit board with two large integrated circuits
Example 4. Printed circuit board with central dissipation.
Example 5. Kapton heater between plates

MODELLING THERMAL RADIATION

Thermal radiation is the electromagnetic radiation emitted by bodies because of its temperature, i.e. not due to radio-nuclear disintegration (like γ rays), not by stimulation with another radiation (like lasers, fluorescent lamps, or X-rays produced with an electron beam), not by electromagnetic resonance in macroscopic conductors (like radio waves). Although radiation with the same properties as thermal radiation can be produced by non-thermal methods (e.g. ultraviolet radiation produced by an electron beam in a rarefied gas, visible radiation produced by chemical luminescence), proper thermal radiation is emitted as a result of the thermal motions at microscopic level in atoms and molecules in macroscopic thermal equilibrium, being almost proportional to the four power of its absolute temperature.

Maxwell's equations of electromagnetism might be used to build a theoretical description of the interaction of electromagnetic radiation with matter, but it is so complicated and uncertain for real bodies (precise knowledge of material data like electrical conductivity, permittivity, and permeability, would be needed), that one has to resort to empirical data in most instances. The theoretical model then is based on Planck's law, with empirical thermooptical values to fit real behaviour of materials. Even so, uncertainty in surface finishing at microscopic level (<10^{-6} m) cannot be avoided in practice, what compromises the accuracy in extrapolating the data. Nevertheless, radiative heat transfer in the extreme near field (<10^{-6} m)

cannot be modelled with Planck's law and requires fluctuational electrodynamics with Maxwell's equations (Nature, DOI: 10.1038/nature16070).

We mainly consider thermal radiation exchanges in vacuum (except when planet atmospheres are considered).

Radiation magnitudes

A propagating radiation has several characteristics (e.g. it propagates in straight line under vacuum and isotropic media), amongst which, a measure of its amount is most important. The basic measure of radiation 'intensity' is irradiance, but several other magnitudes are of interest to characterise radiation 'intensity', each of them showing certain advantages.

Irradiance

Irradiance, E [W/m^2], is defined as the radiant energy flowing per unit time and unit surface (normal to the propagation direction, if not otherwise stated). Irradiance is also the radiation power, Φ, impinging on a unitary surface directly from a source or through intermediate reflections, $E \equiv \mathrm{d}\Phi/\mathrm{d}A$. Irradiance is measured by the effects of the incoming radiation (focused or not) on a detector (thermal effects, or quantum effects).

For one-directional radiation (like sunlight), irradiance depends on surface inclination in the way $E=E_0\cos\beta$; e.g. extra-terrestrial solar irradiation at an astronomic unit (1 au, often written 1 AU), E_0=1370 W/m^2, so that a Sun-facing plate gets that power density, but a 45º tilted plate gets $1370/\sqrt{2} = 969$ W/m^2. Notice that, in general, only a fraction of the irradiance on a surface is absorbed (the absorptance, $\alpha \equiv E_{abs}/E$), the rest being reflected (and, for semi-transparent materials, another fraction is transmitted, the transmittance, $\tau \equiv E_{tra}/E$).

Power

For a given source, the radiation power, Φ [W], is the total power emitted, which can be measured by the energy balance of the source when all other inputs and outputs are known (e.g. within a cryogenic vacuum cavity, to avoid any heat transfer). For other configurations, radiation power is measured in terms of irradiance.

For a point source in non-absorbing media, radiation is isotropic, with irradiance falling with distance from the source such that $\Phi=4\pi R^2 E$, known as the inverse square law. For instance, if we know that at the Sun-Earth distance ($R_{S\text{-}E}$=1 AU) solar irradiance is E_0=1370 W/m^2, solar irradiance at Mars ($R_{S\text{-}M}$=1.5 AU, though Mars-orbit is more elliptic than the Earth's) would be $E=E_0(R_{S\text{-}E}/R_{S\text{-}M})^2=1370\cdot(1/1.5)^2=610$ W/m^2. Notice, however, that irradiance from an infinite planar source does not depend on the distance, and that for an infinite line source, irradiance falls with distance (not distance squared).

Exitance and emittance

For a given distributed source, the total power per unit surface issuing from that surface is termed exitance, M [W/m^2] (formerly called radiosity and denoted by J). For blackbodies, $M=\sigma T^4$, but in a more general case (termed grey bodies), exitance accounts for three different effects: the own emission by

being hot, $\varepsilon\sigma T^4=\varepsilon M_{bb}$, the part reflected from irradiance falling on it, ρE, and the part coming by transmission from the back τE_{rear}, although the latter is absent in opaque objects, and exitances $M=\varepsilon M_{bb}+\rho E+\tau E_{rear}$ is thence:

$$M=\varepsilon M_{bb}+\rho E \tag{14}$$

For a given distributed source, the emittance, M [W/m^2], is the power emitted per unit surface area without accounting for other body inputs, i.e. thermal-radiation emittance is $M=\varepsilon\sigma T^4=\varepsilon M_{bb}$ (known as Stefan's law, with $\varepsilon=1$ in the ideal case of a blackbody). Hence, emittance is that part of exitance not including reflections from incoming radiation (neither transmission from rear-coming radiation). It is ambiguous to use the same symbol M for the whole emerging flux (exitance) and for the part due to own emission (emittance), but so it is the present standard radiometric notation.

For a convex surface source, $\Phi=\int M\mathrm{d}A$ (e.g. for a uniform spherical source of radius R_0, $M=\Phi/(4\pi R_0^2)$, but concave sources emit less power than this area integral because part of it do not escape but feed back the source.

It is difficult to separate the emitted and reflected contribution when measuring exitances; one has to measure with and without shrouds to shield reflections. Close enough to an emitting surface protected from reflections, source emittance equals irradiance on a detector, but, as said above, irradiance decrease with distance in non-planar configurations (with the inverse square law in spherical propagation). For irradiance to be greater than emittance, a converging radiation is needed (i.e. concentration from concave radiators). For instance, a detector close to the Sun surface will get $E=M=\sigma T_S^4=5.67\cdot10^{-8}\cdot5780^4=63\cdot10^6$ W/m^2, decreasing with distance from Sun-centre to probe, R_{Sp}, as $E=M(R_S/R_{Sp})^2$, so that at 1 AU $E=M(R_S/R_{Sp})^2=63\cdot10^6\cdot(0.7\cdot10^9)/(150\cdot10^9))^2=1370$ W/m^2.

Intensity

For a given point source, the power radiated in a given direction, the intensity $I\equiv\mathrm{d}\Phi/\mathrm{d}\Omega$ [W/sr], is important when the source is non-isotropic, since for non-absorbing media, intensity is conservative with the distance travelled (really, the invariant is intensity divided by the index of refraction squared). For a point source $I=\Phi/(4\pi)$. Radiant 'intensity' per unit area, radiance, is much more used than intensity.

Radiance

For extended surfaces (i.e. those that subtend a finite solid angle from the viewer, radiance, L [W/(m^2·sr)], is defined as the energy emerging or impinging on the surface by unit normal area in the viewing direction, unit solid angle, and unit time. Notice that radiance (L) is always measured perpendicular to the viewing direction, and it can be used either for exiting or incoming radiation, whereas exitances and emittance (M) are used only for outgoing radiation, and irradiance (E) is used only for incident radiation; see Fig. 3.

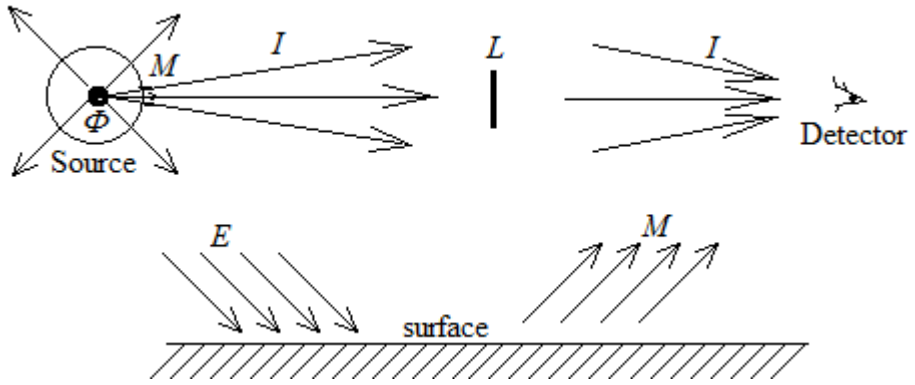

Fig. 3. Different radiation 'intensity' magnitudes. The radiometric and corresponding photometric units are: power Φ [W] or [lm], intensity I [W/sr] or [lm/sr]=[cd], radiance L [W/(m^2·sr] or luminance [lm/(m^2·sr]=[cd/m^2], exitance (or emittance) M [W/m^2] or [lm/m^2]=[lx], and irradiance E [W/m^2] or illuminance [lm/m^2]=[lx].

Radiance, $L \equiv \mathrm{d}^2\Phi/(\mathrm{d}A_\perp \mathrm{d}\Omega)$ [W/(m^2·sr)], is a useful magnitude because it indicates how much of the power issuing from an emitting or reflecting surface will be received by an optical system looking at the surface from some angle of view (the solid angle subtended by the optical system's entrance pupil, like in our eye). The importance of this radiance is also based on its following properties:

- Radiance is isotropic (independent of viewing direction) for perfectly-diffuse surfaces, i.e. for those obeying the cosine dependence of intensity for a fixed un-projected area, like the directional dependence of a flux of photons emanating from a hole in a cavity. If we compare the radiant power exchanged between two surface patches of area $\mathrm{d}A_1$ and $\mathrm{d}A_2$ (or $\mathrm{d}A_{1\perp}$ and $\mathrm{d}A_{2\perp}$, when projected along the centres line), in equilibrium with the isotropic radiation, the radiant power reaching $\mathrm{d}A_2$ from $\mathrm{d}A_1$ must be equal to the radiant power reaching $\mathrm{d}A_1$ from $\mathrm{d}A_2$:

$$\left.\begin{aligned} \mathrm{d}^2\Phi_{12} &= L_1(\beta_1)\,\mathrm{d}A_{1\perp}\mathrm{d}\Omega_{12} = L_1(\beta_1)\,\mathrm{d}A_{1\perp}\left(\frac{\mathrm{d}A_{2\perp}}{r_{12}^2}\right) \\ \mathrm{d}^2\Phi_{21} &= L_2(\beta_2)\,\mathrm{d}A_{2\perp}\mathrm{d}\Omega_{21} = L_2(\beta_2)\,\mathrm{d}A_{2\perp}\left(\frac{\mathrm{d}A_{1\perp}}{r_{12}^2}\right) \end{aligned}\right\} \mathrm{d}^2\Phi_{12} = \mathrm{d}^2\Phi_{21} \Rightarrow L_1(\beta_1) = L_2(\beta_2) \qquad (15)$$

  and, since they are at equilibrium, we arrive at the radiance isotropy, $L(\beta_1)=L(\beta_2)$ for any β. This means that for an ideal radiator (the blackbody introduced below), and with more or less approximation for many practical radiators (in the limit of perfect diffusers), the power radiated in a given direction per unit radiating area projected along the view path is L for any direction (it would be $L\cos\beta$ if the area were not projected, β being the zenith angle of the direction considered. Any surface that radiates (by own emission or by reflection from other sources) with a directional intensity following this cosine law is named 'perfect diffuser' or Lambertian surface, in honour of J.H. Lambert's 1760 "Photometria". A radiation detector pointing to a Lambertian planar surface detects the same irradiance when pointing at any position because the projected area at a given distance is constant (only depends on the aperture of the detector); it sees uniform radiance because, although the emitted power from a given area element is reduced by the cosine of the emission angle, the size of the observed area is increased by a corresponding amount.

- Radiance is simply related to exitances in a Lambertian surface by $L=M/\pi$, as deduced from its definition, $L\equiv \mathrm{d}^2\Phi/(\mathrm{d}A_\perp \mathrm{d}\Omega)$, and $\Phi=\int M\mathrm{d}A$:

$$\Phi=\int_A M\mathrm{d}A=\int_A\int_\Omega L\mathrm{d}A_{proj}\mathrm{d}\Omega \quad\rightarrow\quad M=\int_0^{2\pi} L\cos(\beta)\mathrm{d}\Omega=L\int_0^{\pi/2}\cos(\beta)2\pi\sin(\beta)\mathrm{d}\beta=\pi L \tag{16}$$

- Radiance is conserved in non-dissipative optical systems (really, radiance divided by the index of refraction squared is invariant in geometric optics), as dictated by an energy balance, i.e. radiance at the source is the same that at the detector (e.g. if one takes a picture of the Sun disc, the light-intensity received by any illuminated pixel on the detector will be the same, independently of the distance to the Sun).

Radiance of a non-uniform source, like a half moon reflexion, depends on the viewing point (direction and distance), whereas radiance of a uniform source like the Sun, does not depend on direction or distance. Looking from the Sun to the Earth, a small patch of 1 m^2 at the Sun surface emits $L=M/\pi=\sigma T_S^4/\pi=63\cdot10^6$ W/m^2/$\pi=20\cdot10^6$ W/(m^2·sr), i.e. $20\cdot10^6$ W per unit solid angle towards its frontal direction (in other directions, this patch emits with the cosine law; e.g. zero in the tangential direction). At the mean Sun-Earth distance, $R_{SE}=150\cdot10^9$ m, a 1 m^2 frontal patch subtends a solid angle from the Sun of $\Omega=(1\ m^2)/R_{SE}^2=1/(150\cdot10^9)^2=44\cdot10^{-24}$ sr (the whole Earth subtends $\Omega=\pi R_E^2/R_{SE}^2=5.7\cdot10^{-9}$ sr from the Sun, or $2R_E/R_{SE}=85\cdot10^{-6}$ rad, and the Sun from the Earth $\Omega=\pi R_S^2/R_{SE}^2=68\cdot10^{-6}$ sr, or $2R_S/R_{SE}=0.01$ rad), so that the 1 m^2 frontal patch at the Earth gets $L\Omega=20\cdot10^6\cdot44\cdot10^{-24}=0.9\cdot10^{-15}$ W from the 1 m^2 frontal patch at the Sun. If we add up the contribution from the whole solar disc, we get $L\Omega\pi R_S^2=20\cdot10^6\cdot44\cdot10^{-24}\pi(0.7\cdot10^9)^2=1370$ W/m^2 for the irradiation on a 1 m^2 facing panel at the Earth (outside the atmosphere).

Blackbody radiation

Considering an evacuated material enclosure (of any material property, but non-interacting with the environment, i.e. opaque) at thermodynamic equilibrium (i.e. isothermal), and the EM radiation field created inside by the thermal vibrations of atoms at the walls, thermodynamic equilibrium between matter and radiation dictates that this radiation (named blackbody radiation by Gustav Kirchhoff in 1860) must have the following properties:

1. Temperature. One may ascribe a temperature to the radiation, the temperature of the enclosure.
2. Isotropy. The radiation must be isotropic (i.e. a detector cannot discern any privileged direction).
3. Photon gas. By quantum physics, energy is quantized, $E=h\nu=hc/\lambda$ ($h=6.6\cdot10^{-34}$ J·s) and the EM waves can be viewed as EM particles, called photons. One often refers to the photon gas as an ideal gas (i.e. a set of non-interacting particles, each with an energy $E=h\nu$); the main distinction between the photon gas and the traditional ideal gas being that photons are not conservative and that they all move at the speed of light, c, but with different wavelengths, whereas particles in a classical gas are conservative and have the Maxwell-Boltzmann distribution law for speeds.
4. Spectrum. In similarity with the fact that maximum entropy yields the Maxwell-Bolzmann distribution of molecular speeds in classical gases, maximum entropy yields the Planck

distribution of photon wavelengths or frequencies for blackbody radiation. Planck's law in terms of spectral energy density [(J/m^3)/m] is:

$$u_\lambda = \frac{8\pi hc}{\lambda^5\left[\exp\left(\frac{hc}{k\lambda T}\right)-1\right]} \qquad (17)$$

The number of photons per unit volume with energy $E=h\nu=hc/\lambda$ between λ and $\lambda+\mathrm{d}\lambda$ is u_λ/E. Although the wavelength-range extends in principle to the whole domain, $0<\lambda<\infty$, Planck's distribution is very peaked, particularly at lower wavelengths, and 93% of the whole energy lies in the range $0.5<\lambda/\lambda_{\mathrm{Mmax}}<4$, where $\lambda_{\mathrm{Mmax}}=C/T$ and $C=2.9.10^{-3}$ m·K. Human eye can only see in the range, $0.4<\lambda/\mu\mathrm{m}<0.7$ (the so called visible range, which can be subdivided in six 0.5 μm amplitude colour bands corresponding to violet, blue, green, yellow, orange, and red, in increasing order.

5. Emission. When this radiation escapes through a small hole in the enclosure (small holes appear black to the eye because they do not reflect any illuminating light), Planck's law in terms of spectral exitance [(W/m^2)/m] is:

$$M_\lambda = \frac{c_1}{\lambda^5\left[\exp\left(\frac{c_2}{\lambda T}\right)-1\right]} = \frac{2\pi hc^2}{\lambda^5\left[\exp\left(\frac{hc}{k\lambda T}\right)-1\right]} = \pi L_\lambda \qquad (18)$$

where L_λ is the spectral radiance [(W/m^2)/sr], and $c_1=3.74\cdot10^{-16}$ W·m^2, $c_2=0.0144$ m·K. Recall: $h=6.626\cdot10^{-34}$ J·s, $k=1.38\cdot10^{-23}$ J/K. Notice that exitance and emittance are referred to real surface area, whereas radiance is referred to the projection of the emitting area in that direction; thence, an infinitesimal emitter of area dA emits with a cosine law (projected area) but is seen with a constant radiance at all 2π steradians, with, $M_\lambda = \int L_\lambda \cos\beta d\Omega = \int L_\lambda \cos\beta 2\pi \sin\beta d\beta = \pi L_\lambda$. Further notice that it is wrong to substitute there $\lambda=c/\nu$; the correct relation is $\mathrm{d}L=L_\lambda\mathrm{d}\lambda=L_\nu\mathrm{d}\nu$, i.e.:

$$dL = \frac{2hc^2}{\lambda^5\left[\exp\left(\frac{hc}{k\lambda T}\right)-1\right]}\mathrm{d}\lambda = \frac{2h\nu^3}{c^2\left[\exp\left(\frac{h\nu}{kT}\right)-1\right]}\mathrm{d}\nu \qquad (19)$$

Planck's law corollaries:

- Wien's displacement law: $\lambda_{Mmax}=C/T$, with $C=2.8978\cdot10^{-3}$ m·K$=hc/(kx)$, where x is the root of $x=5(1-\mathrm{e}^{-x})$ (=4.965). Notice again the rapid spread of Planck's distribution with representative wavelength: at the peak, $\lambda T=C$, the spectral emission falls with the fifth power of λ_{Mmax}.
- Stefan-Boltzmann's law: $M=\int M_\lambda\mathrm{d}\lambda=\sigma T^4$, proposed by Jozef Stefan in 1879 and deduced by his student Ludwig Boltzmann in 1884, with $\sigma=2\pi^5k^4/(15c^2h^3)=5.67\cdot10^{-8}$ W/(m^2·K^4) being the Stefan-Boltzmann constant. Stefan used this law to find for the first time the temperature of the Sun.

Planck's law approximations:

- In the limit of short wavelengths, it reduces to Wien's law: $M_\lambda = \dfrac{c_1}{\lambda^5 \exp\left(\dfrac{c_2}{\lambda T}\right)}$.
- In the limit of long wavelengths, it reduces to Rayleigh-Jeans law: $M_\lambda = \dfrac{2\pi ckT}{\lambda^4}$.

Why exponent 4 in blackbody radiation?

Using the kinetic theory of an ideal gas composed of particles with momentum $\vec{p}$ (of modulus $|p|$; not to be confused with p for pressure):

- Kinetic theory teaches that pressure (p) on a surface is twice the momentum ($2|p|$), times the speed (c), times the number of collisions per unit area and time ($n/6$, $n=N/V$ being the number of particles per unit volume, and 1/6 the fraction moving towards our surface); i.e. $p=(1/3)nc|p|$.
- Wave-particle duality teaches that, for a photon, $E=h\nu=\lambda|p|\nu=c|p|$. In relativistic mechanics, in order to be conserved, momentum must be defined as $\vec{p} \equiv \gamma m_0 \vec{v}$, and kinetic energy is $E^2=|p|^2c^2+m^2c^4$, or for a zero-rest-mass particle, $E=|p|c=c|p|$.
- Consequently, radiation pressure is $p=(1/3)nc|p|=(1/3)nE=(1/3)u$, $u=U/V$ being the internal energy per unit volume. Notice the difference between $p=(1/3)U/V$ for a photon gas, and $p=(\gamma-1)U/V$ for a perfect gas ($U=nc_vT$+const$=nRT/(\gamma-1)$+const$=pV/(\gamma-1)$+const). It follows that $\gamma_{\text{photons}}=4/3=1.33$.
- Hence, pressure in a photon gas only depends on temperature (not in V or N; it would be 100 kPa at 107 000 K), whereas in an ideal gas pressure depends on T and V (or N).
- But Thermodynamics teaches that $\mathrm{d}U=T\mathrm{d}S-p\mathrm{d}V$, so that dividing by $\mathrm{d}V$ and fixing T, and with Maxwell relation from $\mathrm{d}A=-S\mathrm{d}T-p\mathrm{d}V$:

$$\left.\frac{\partial U}{\partial V}\right|_T = T\left.\frac{\partial S}{\partial V}\right|_T - p = T\left.\frac{\partial p}{\partial T}\right|_V - p \overset{U=uV}{=} \overset{p=\frac{u}{3}}{u} = \frac{T}{3}\left.\frac{\partial u}{\partial T}\right|_V - \frac{u}{3} \qquad (20)$$
$$\Rightarrow \quad \frac{\mathrm{d}u}{\mathrm{d}T} = \frac{4u}{T} \quad \Rightarrow \quad u = aT^4$$

- To compare the photon gas with the ideal gas, the equation above can be rewritten as:

$$\left.\frac{\partial \ln p}{\partial \ln T}\right|_V = 1 + \frac{1}{p}\left.\frac{\partial U}{\partial V}\right|_T \quad \rightarrow \begin{cases} \text{ideal gas } U = nc_vT & \Rightarrow \left.\dfrac{\partial U}{\partial V}\right|_T = 0 \quad \Rightarrow \left.\dfrac{\partial \ln p}{\partial \ln T}\right|_V = 1 \\ \text{photon gas } U = 3pV & \Rightarrow \left.\dfrac{\partial U}{\partial V}\right|_T = 3p \quad \Rightarrow \left.\dfrac{\partial \ln p}{\partial \ln T}\right|_V = 4 \end{cases} \qquad (21)$$

and that is the answer to the question of why a photon gas has $u=aT^4$ and the ideal gas has $u=bT$: because at a given temperature, pressure in an ideal gas does not contribute to energy, whereas pressure in a photon gas is proportional to energy in the form $p=(1/3)u$.

Blackbody spectral fraction. Computing the fraction of blackbody radiation within a spectral band is important is many applications, what can be helped by the mathematical equality (obtained by integrating by parts a series expansion of Plank's law):

$$F_{0-\lambda} \equiv \frac{1}{\sigma T^4}\int_0^{\lambda} \frac{c_1 \mathrm{d}\lambda}{\lambda^5\left[\exp\left(\frac{c_2}{\lambda T}\right)-1\right]} = \frac{15}{\pi^4}\sum_{n=1}^{\infty}\left[\frac{e^{-x}}{n^4}\left(x^3+3x^2+6x+6\right)\right] \text{ with } x \equiv \frac{nc_2}{\lambda T} \qquad (22)$$

Two infinite blackbodies in a parallel-plate configuration exchange a heat flux of $\dot{q}_{ij} = \sigma\left(T_j^4 - T_i^4\right)$. Radiation-exchange between real bodies is modelled by introducing separate directional and spectral factors when possible (only for isothermal diffuse surfaces with only two spectral bands of interest), or by statistical ray tracing modelling in the more general case (using Monte Carlo method).

Exercise 4. A manufacturer of electrical infrared heaters quotes in the applications of its products a maximum heating power of 1.2 MW/m^2. What can be deduced about the operation temperature of its heaters?

Ans.: Assuming the heater elements to be black-bodies, from $\dot{q} = \sigma\left(T^4 - T_0^4\right)$, we deduce $T = \left(T_0^4 + \dot{q}/\sigma\right)^{1/4} = \left(300^4 + 1.2\cdot10^6 \big/ \left(5.67\cdot10^{-8}\right)\right)^{1/4}$ =2145 K (1870 ºC). There are some heater elements close to black-bodies, as carbon heaters, whereas typical industrial heaters use kanthal wire (an iron-chromium alloy), which has an emissivity ε=0.7, and would need to be operated at 2300 K to yield that power, what is not realistic because its melting temperature is below 2000 K. There are, however, other metals withstanding higher temperatures (wolfram works above 3000 K in halogen lamps), but they are much more expensive and difficult to work with: they oxidise quickly, they are brittle, etc.

Notice that one may understand the heating power as the emittance, i.e. $\dot{q} = \sigma T^4$, because, at high temperatures the difference is imperceptible, $T = \left(\dot{q}/\sigma\right)^{1/4}$ =$(1.2\cdot10^6/(5.67\cdot10^{-8})^{1/4}$=2145 K (1870 ºC), but for lower heating powers the difference may be inadmissible (e.g. which temperature must have a heater for $\dot{q}$=1 kW/m^2, $T = \left(T_0^4 + \dot{q}/\sigma\right)^{1/4}$ = 128 ºC or $T = \left(\dot{q}/\sigma\right)^{1/4}$ =91 ºC?).

Real bodies: interface

The ideal blackbody model is in essence an interface model, describing the radiation entering or leaving a small hole in a cavity. The interaction of thermal radiation with real bodies departs from the blackbody model in several respects:

- At the surface (i.e. an interface with abrupt change in refractive index). Real bodies do not absorb all the incident energy because there is some reflection and some transmission. If the transmitted energy is totally absorbed shortly within the body (say in less than 1 mm), the body is said to be opaque, and the absorption process can be ascribed to the interface, calling 'absorptance' the fraction of the incident energy absorbed (i.e. not reflected back). As a consequence of the energy balance, a partially absorbing surface must be partially emitting, i.e. at the same temperature, real bodies emit less energy than black-bodies, what is quantified by the factor named emissivity. See thermo-optical surface properties data.
- At the bulk (of a constant or slowly varying refractive index media). Real bodies transmit radiation energy with some absorption (intensity decays exponentially along the path), and some scattering (re-radiation at the same or different wavelength in other directions than the path).

According to the decay length, substances are grouped into two limit cases: opaque materials (if the decay length is less than the thickness of interest, and transparent materials (if the decay length is much larger than the thickness of interest); for instance, a 20 nm gold layer (deposited on a transparent substrate) is transparent enough to see through it (it has 20% transmittance in the visible range).

One should always keep in mind that ascribing physical properties to a geometrical surface is just a simplifying limit; in reality, like in a blackbody cavity, radiant energy is absorbed or emitted within a sizeable thickness, not just at a geometrical surface.

Emissivity

Real surfaces emit less energy than the ideal blackbody at the same temperature, what can be measured by an energy balance test in a non-equilibrium arrangement (e.g. within a cryogenic vacuum chamber). Spectral emissivity is defined in detail as the fraction of spectral radiance in a given direction, relative to blackbody radiance under the same conditions:

$$\varepsilon_{\lambda T\beta\theta} \equiv \frac{L_{\lambda T\beta\theta}}{L_{\lambda T,\mathrm{bb}}} \tag{23}$$

whereas spectral hemispherical emissivity is defined in terms of emittance:

$$\varepsilon_{\lambda T} \equiv \frac{M_{\lambda T}}{M_{\lambda T,\mathrm{bb}}} = \frac{\int_0^{2\pi}\int_0^{\pi/2} L_{\lambda T\beta\theta}\cos\beta\sin\beta\,\mathrm{d}\beta\mathrm{d}\theta}{\int_0^{2\pi}\int_0^{\pi/2} L_{\lambda T,\mathrm{bb}}\cos\beta\sin\beta\,\mathrm{d}\beta\mathrm{d}\theta} = \frac{\int_0^{2\pi}\int_0^{\pi/2} \varepsilon_{\lambda T\beta\theta}\cos\beta\sin\beta\,\mathrm{d}\beta\mathrm{d}\theta}{\pi} \tag{24}$$

and if there is azimuthal symmetry $\varepsilon_{\lambda T} = 2\int_0^{\pi/2} \varepsilon_{\lambda T\beta\theta}\cos\beta\sin\beta\,\mathrm{d}\beta$. A total hemispherical value can be defined by:

$$\varepsilon_T \equiv \frac{M_{\lambda T}}{M_{\lambda T,\mathrm{bb}}} = \frac{\int_0^{\infty} M_{\lambda T}\mathrm{d}\lambda}{\int_0^{\infty} M_{\lambda T,\mathrm{bb}}\mathrm{d}\lambda} = \frac{\int_0^{\infty} \varepsilon_{\lambda T\beta\theta} M_{\lambda T,\mathrm{bb}}\mathrm{d}\lambda}{\sigma T^4} \tag{25}$$

where spectral emittance and radiance for a blackbody, $M_{\lambda T,\mathrm{bb}}$ and $L_{\lambda T,\mathrm{bb}}$, were given by (10). When emissivity does not change with direction, $L_{\lambda T\beta\theta}/L_{\lambda T}$, it is termed diffuse emission or Lambertian emission. In that case, the emitted power flux varies proportionally to the projected area of emission, i.e. with the cosine law, $M_\beta = M_0\cos\beta$; a hot spherical surface is seen with a uniform flat brightness due to area compensation; however, a metallic hot sphere appears darker at the centre because metal emissivity is greater towards the horizon, whereas hot non-metal spheres look brighter at the centre because emissivity of dielectrics tends to zero at levelling angles. Blackbody emission verifies Lambert's cosine law.

Unless otherwise stated, emissivity values refer to quasi-total hemispherical values where the integration the integration in (15) is restricted to the far infrared band, 3 μm<λ<30 μm, and the emitting surface is at near room temperature, T≈300 K. Emissivity dependence with temperature and direction is often negligible, but variations with wavelength may be important.

- Non-metals emit in the infrared nearly as blackbodies (say ε>0.8), irrespective of structure or apparent visible colour (e.g. white paint emits nearly the same as black paint, and the same for human race skin colours). Directional emissivity tends to zero at level directions. In the case of transparent coatings in the infrared, actual emissivity of a coated surface depends on emissivity of the substrate.
- Metal emissivity varies a lot with surface state (ε<0.1 for polished metals, to ε>0.8 if hard oxidised), with direction of measurement (it is maximum near level directions, says at β≈80º, sharply decreasing to zero at level directions, β=90º), with temperature (slowly increases), and with wavelength. For wolfram (tungsten), total hemispherical emissivity increases from ε=0.09 at 300 K to ε=0.39 at 3000 K (with a large spectral slope; at 3000 K, ε_λ=0.45 at λ=0.5 μm and ε_λ=0.20 at λ=4 μm). Notice that the short-wave radiation emitted by a lamp bulb (and quartz covered heaters) is limited by the transmittance of the protection (normal glass bulbs have a cut-off at 3 μm, and quartz bulbs at 5 μm with a dip in transmittance at 2.8 μm).

Absorptance

When a material surface at temperate T is exposed to monochromatic beam along a direction (β,θ) of radiance $L_{\lambda\beta\theta}$ (irradiance $\mathrm{d}E_{\lambda\beta\theta}=L_{\lambda\beta\theta}\mathrm{d}\Omega$; notice that they are independent of surface conditions), only a fraction $\alpha_{\lambda T\beta\theta}$ is absorbed (increasing internal energy; now dependent on surface conditions). Reversibility of detailed thermodynamic equilibrium implies:

$$\alpha_{\lambda T\beta\theta}=\varepsilon_{\lambda T\beta\theta} \quad \text{Kirchhoff 's law}\,(1859) \tag{26}$$

since, if one considers an element of a real surface as part of a blackbody cavity (i.e. in equilibrium at uniform temperature), the isotropy preservation of blackbody radiation and the local energy balance implies that $\alpha_{\lambda T\beta\theta}E_{\lambda T\beta\theta}=\varepsilon_{\lambda T\beta\theta}M_{\lambda T\beta\theta}$ and $E_{\lambda T\beta\theta}=M_{\lambda T\beta\theta}$ for a blackbody.

Spectral hemispherical absorptance is then:

$$\alpha_{\lambda T}=\frac{\int_0^{2\pi}\int_0^{\pi/2}\alpha_{\lambda T\beta\theta}L_{\lambda\beta\theta}\cos\beta\sin\beta\,\mathrm{d}\beta\,\mathrm{d}\theta}{\int_0^{2\pi}\int_0^{\pi/2}L_{\lambda\beta\theta}\cos\beta\sin\beta\,\mathrm{d}\beta\,\mathrm{d}\theta} \tag{27}$$

and if the incident radiation is diffuse and there is azimuthal symmetry in the absorptance, $\alpha_{\lambda T}=2\int_0^{\pi/2}\alpha_{\lambda T\beta}\cos\beta\sin\beta\,\mathrm{d}\beta$. A total hemispherical value can be defined in terms of the spectral irradiance shining on the surface:

$$\alpha_T \equiv \frac{\int_0^\infty \alpha_{\lambda T} E_\lambda \mathrm{d}\lambda}{\int_0^\infty E_T \mathrm{d}\lambda} \qquad (28)$$

Unless otherwise stated, absorptance values refer to normal incidence solar radiation, i.e. approximately to incident blackbody radiation at 5780 K (0.3 μm<λ<3 μm, or 0.1 μm<λ<3 μm if the extra-terrestrial UV band is included), since absorptance in the far infrared band is almost equal to emissivity in the far infrared (equal for monochromatic radiation, from Kirchhoff's law). From what is said under Emissivity, far IR absorptance values are almost unity for non-metal surfaces (except in case they are transparent in the IR), whereas polished metal surfaces reflect most part of far IR radiation. For opaque surfaces in general, what is not reflected is absorbed: $\alpha=1-\rho$. Water absorbs practically all at 3 μm, PVC at 3.5 μm.

Reflectance

Real surfaces reflect part of the incident irradiation, ρ, which can be measured with a radiometer, first measuring the irradiance (radiant flux incident on the surface by unit area, E), and thence the radiance (radiant flux exiting the surface by unit area and unit solid angle, L). For a Lambertian surface, $\rho=\pi L/E$, but for real surfaces, reflectance depends on both, the incoming and outgoing directions considered (as well as on wavelength and surface temperature). Preservation of the isotropy in the interaction of a real surface with blackbody radiation dictates that bidirectional spectral reflectance at a given wavelength is the same when both directions (incident and reflected) are exchanged, i.e. $\rho_{\lambda\beta\theta T\beta'\theta'}=\rho_{\lambda\beta'\theta' T\beta\theta}$. Detailed reflectance measurements are computed by dividing the increment of exitance from a real surface by the irradiance used for the probing.

For opaque surfaces in general, what is not absorbed is reflected: $\rho=1-\alpha$. Transparent surfaces reflect a small fraction of incident radiation due to the difference in refractive index: $\rho=(n_1-n_2)^2/(n_1+n_2)^2$; e.g. in the visible band, for common glass in air, $n_1=1$, $n_2=1.5$ and $\rho=0.04$; in the far infrared band (i.e. around $\lambda=10$ mm), for germanium in air, $n_1=1$, $n_2=4$ and $\rho=0.36$.

Reflection at real surfaces always has some scattering. Several limit cases are of most interest:

- Specular reflection, when there is no scattering and the reflected ray has an opposite angle to the incident ray, relative to the surface normal, $\beta_1=-\beta_2$. Mirrors approach this behaviour. Polished metals are good mirrors in the visible, infrared and microwave bands, although common mirrors are not first-surface mirrors but second-surface mirrors where a metal coating (silver in most cases) is behind a transparent glass sheet.
- (Perfect) Diffuse reflection, when reflectance is uniform for all outgoing direction. The reflected power flux varies proportionally to the projected area of emission, i.e. with the cosine law, $M_\beta=M_0\cos\beta$. When a planar surface of such a perfect diffuser is illuminated by a beam in any direction, the surface appears uniformly illuminated, due to area compensation, however, in the case of an illuminated curved surface, it appears brighter in the regions where the shining beam falls more perpendicular (e.g. a frontally illuminated sphere appears brighter at the centre; the

Moon is not a perfect diffuser, as explained below). Spectralon®, used in optical metrology and as a reference surface in remote sensing, is a fluoropolymer with nearly perfect diffuse reflectance to solar radiation (ρ>0.99 from 400..1500 nm, and ρ >0.95 in the whole range from 250 nm to 2500 nm; but ρ<0.2 for λ>5.4 μm).

- Retro-reflection, when the reflected ray goes out precisely in the same direction than the incident ray. The fact that the Moon is seen almost uniformly illuminated by the Sun at full Moon (instead of being brighter at the centre as for a perfect diffuser), is explained by the retro-reflective properties of lunar dust.
- Advanced shading models. Several shading models have been lately developed for computer graphics, to better match real directional reflectance data. For heat transfer problems, the perfect diffuser model is sometimes enhanced to a two-term reflection model: a (perfect) diffuser reflectance, plus a specular reflectance.

Transmittance

Transmittance at an interface is the fraction of incident radiation energy that propagates to the rear of the interface, always with a change in direction (from the incident direction), which can be collimated (refraction), or scattered. An energy balance indicates that, at any interface, absorptance plus reflectance plus transmittance must equal unity, $\alpha+\tau+\rho=1$.

Real bodies: bulk

Bulk effects on radiation-matter interaction are rarely considered in spacecraft thermal control, where the model of opaque surfaces is the rule; only a few cases of transparent materials are used in STC, notably second surface mirrors, and viewing windows in vehicles and space suits.

Absorptance and transmittance

Radiation absorption and transmission are bulk processes (ascribed to the surface when the penetration distance is very small). When considering bulk behaviour, instead of reflection (re-transmission backwards) one considers scattering, which is the re-transmission in all directions (backward and forward) except in the prolongation of the incoming ray, which is termed transmission. Hence, the energy balance establishes that absorption plus scattering plus transmission equals unity.

Absorption (or better, transmission) within a medium is characterised by an attenuation or extinction coefficient, α, (be careful to avoid confusion with surface absorptance with the same symbol; now α has dimensions of m^{-1}), such that radiation intensity falls exponentially along the path as $I(x)=I_0\exp(-\alpha x)$, what is known as Beer-Lambert's law. The extinction factor includes the effect of absorption and scattering, and is a function of wavelength. A layer of pure water seems transparent (and indeed some blue rays may penetrate 100 m down the surface), but it absorbs all infrared radiation in the first millimetre (except when it impinges at level angles).

For finite thickness, the optical depth, τ, is defined by $I_{out}=I_{in}\exp(-\tau)$, and depends on wavelength. Clear sky has a total optical depth of 0.35 along the vertical path; aerosols increase the optical depth, making the Sun difficult to locate when τ>4. In engineering problems however, it is still common to talk about

absorptance and transmittance factors (not coefficients) when dealing with finite transparent materials, and apply $\alpha+\tau+\rho=1$ globally.

When transmission occurs in a collimated way, it is termed refraction, and the ray directions verify Snell's law, $n_1 \sin\beta_1 = n_2 \sin\beta_2$, where n is the refractive index and β the angle with the normal to the interface. Other times, transmission is not collimated but scattered, losing the ability to form images (the material is then said to be translucent).

Scattering

In general, scattering is the process in which particles (material or electromagnetic) travelling along a given direction are deflected as a result of collision (interaction) with other particles (material particles). Electromagnetic scattering can be due to different processes, classified as elastic and non-elastic.

- Elastic scattering, where the wavelength is preserved. It may take place under several circumstances:
  - At interfaces, what gives way to diffuse reflection.
  - At molecular level in the medium, what is known as Rayleigh scattering. The scattered pattern is lobular symmetric (i.e. axisymmetric and symmetric to the normal plane), and the intensity is proportional to λ^{-4} (i.e. scatters more the lower the wavelength, what gives way to the bluish of our atmosphere and oceans),
  - At particles comparable in size to the radiation-wavelength, what is known as Mie scattering (G. Mie solved in 1908 Maxwell equations for the interaction of an EM-wave with a dielectric sphere) or Tyndall's effect (J. Tyndall was the first to attribute in 1859 the bluish of the sky by selective scattering, later explained by Rayleigh). The scattered pattern is lobular non-symmetric, larger forward, with intensity independent of frequency.
- Non-elastic, where the wavelength changes, like in Raman scattering at molecular level.

Measuring thermal radiation

Electromagnetic radiation is characterised by its energy amount (J/m^3 if standing, or W/m^2 if propagating), its oscillation frequency, ν (or wavelength, λ, with $\lambda=(c/n)/\nu=\lambda_0/n$), and other parameters of little interest for thermal radiation, like polarization, coherence, pressure, etc.

Radiometers measure the amount of radiation coming from a field of view and falling onto a detector. The field of view (FOV) is delimited by a series of holes, or focused by refractive lenses, or mirror reflectors. The incoming radiation may be due to emission by objects in the FOV, by reflection on them from other bodies, and by transmission through matter from the background). We only deal here with thermal radiation, and thermal detectors are described below. Detectors for shorter-wavelength radiations may be photographic films (for visible, ultraviolet, X-rays), supersaturated phase-change media (e.g. Wilson cloud chamber), gas-discharge devices (e.g. Geiger counter), etc. Detectors for longer-wavelength radiations are resonant electrical circuits known as aerials or antennas, with size proportional to wavelength, and sometimes with a reflector to concentrate the EM-field to be detected.

The primary standard (the World Radiometric Reference, from the World Meteorological Organization) is based on absolute cavity radiometers. An absolute radiometer consist of a black cavity with an absorber connected to a heat sink through a precision heat flux transducer (a thermopile), upon which two beams can be directed using appropriate shutters: the sample irradiance to measure (e.g. a solar beam), and a calibrated beam from a radiant electrical heater, controlled to maintain the same heat flux with and without the sample beam. In other versions, two opposite cavities are used, connected through the heat-flux assembly; if P_{shut} is the heater power with the sample beam shut, and P_{open} the power when sampling, the total beam irradiance is found from $E=k(P_{shut}-P_{open})$, with k obtained from $E_{ele}=kP_{shut}$, with E_{ele} and P_{shut} measured. As for any electronic sensor, periodic calibration is needed (against a controlled blackbody cavity).

Thermal radiometers can be classified on different basis: type of detector, spectral range, directional range, array size, etc.

Infrared detectors

According to detector type, measuring thermal radiation can be based on different effects:

- Thermal effects. Incoming radiation is focused on a thermal detector (a tiny blackened electrical thermometer), whose temperature variation is measured. Two thermometric effects can be used: electric resistance (with a tiny thermistor called 'bolometer'), and thermoelectric voltage (a series array of thermocouples called 'thermopile'). For a given irradiation, the response is the same for any spectral distribution, but as emissive power falls rapidly with falling temperature, thermal detectors are not suitable for low temperatures. Thermal detectors are the most common for total thermal radiation, but used to have lower sensitivity and response time than quantum detectors; nowadays, thermistors and thermopiles made by metal deposition are bridging the gap. The response of thermal detectors depends on the temperature of the detector's body and supports, which must be tightly controlled.
- Quantum or photon effect. Incoming radiation causes an electric charge release that is measured by photovoltaic, photoelectric, or photoconductive effects. Quantum effect detectors have an upper bound in wavelength response, and work best in a narrow waveband just below that cut-off wavelength, were sensibility is much greater than for thermal detectors. For a given irradiation power, E, the response is proportional to the number of photons, and thus to λ, since $E=Nh\nu=Nhc/\lambda$=constant. Quantum-effect detectors are based on electron transitions in semiconductors, notably in the valence band of CdTe-HgTe alloys (known as HgCdTe), which requires cryogenic cooling for good signal-to-noise ratio, and more recently in the conduction well in GaAs.
- Optical effects. Incoming radiation is visually compared with radiation emitted by a calibrated source (optical pyrometer).
- Chemical effects. Incoming radiation cause a chemical reaction. Since thermal radiation is not very energetic, it only applies to visible and near infrared detection in special photographic film.

According to spectral range:

- Total radiometers. They measure total radiation (i.e. the integral effect of all wavelengths, always limited by the optics). Sometimes, detectors with narrow-band sensitivity are used to infer total radiation.
- Spectro-radiometers. They measure in a narrow spectral band, selected by appropriate spectral filters, or a polychromators (dispersion in a prism or in a fibre optic, or diffraction in a diffraction grating) and special filters (resulting in a monochromator device).
  - In the near IR band (say 0.7..1.4 μm. Silicon, germanium, indium-gallium arsenide (InGaAs), or photographic detectors, can be used (IR-CCD since 1978). In this range, SiO_2 has high transmittance (used in fibre optics), and water has low absorption. Used for night vision with CCD image intensifiers, and for spectroscopic analysis. Quartz windows are used. Notice that sometimes near-IR lighting is used as an active means to enhance night vision.
  - In the short or middle IR band (say 3..5 μm, centred around the first atmospheric window), indium antimonide (InSb), lead selenide (PbSe), or mercury cadmium telluride (HgCdTe) detectors can be used. Sapphire windows are used. With these kinds of detectors, IR-guided missiles follow the thermal signature left by aircraft (the exhaust nozzle and plume are at some 1000 K).
  - In the long or far IR band (say 8..14 μm, centred around the main atmospheric window), HgCdTe detectors are used, which work in a broad infrared band including the middle IR. Germanium windows are used. Mercury Cadmium Telluride (MCT) is a photoconductive alloy of CdTe and HgTe; CdTe is a semiconductor with a bandgap of approximately 1.5 eV at room temperature. HgTe is a semi-metal, hence its bandgap energy is zero, so that by selecting the composition one may tune the optical absorption of the sensor to the desired infrared wavelength. MCT is expensive, difficult to get in good homogeneity, and must be operated at cryogenic temperatures (below 100 K). A recent substitute of MCT (less expensive but with lower performances) is gallium arsenide (GaAs).

According to field of view (directional range):

- Normal radiometers. They measure radiation coming from a narrow field of view. In the case of solar radiation they are known as pyroheliometers.
- Hemispherical radiometers. Only used to measure total solar radiation at ground level, for meteorological or solar-energy applications. They are known as pyranometers (see below).

According to the temperature range of the object:

- Pyrometers, if especially suited to high temperature measurement.
- Radiometers. In general.

According to the spatial scanning:

- Point radiometers. They use one single sensor (belonging to one of the mentioned types) to yield a single spatial measurement of radiation or the associated temperature.

- Thermal cameras (or thermo-cameras, or infrared cameras). They yield a two-dimensional measurement. Old devices (up to 1970) were based on a mechanical 2-D scanner and a point radiometer; others used a linear array of sensors and 1-D mechanical scanning, while modern ones (since 1980s) use a 2-D array of sensors electrically scanned; the most accurate and quick-response IR sensors use HgCdTe detectors at cryogenic temperature, but they are very expensive and difficult to maintain. More recent technology was based on monolithic CMOS focal plane arrays of InSb or InGaAs. The newest cameras are based on uncooled micro-bolometers (see below); they are cheaper, smaller, consume less power, and require no cooling time (although they must be temperature-stabilised for proper accuracy). Micro-bolometer cameras are used for accurate temperature measurement, but their resolution is currently limited to 0.5 mega-pixel (640×480). Older pyroelectric CCDs have better spatial resolution and response time, but lack accuracy, and need periodic chopping) can be used for more qualitative work (e.g. night vision). Thermography is synonymous of IR imaging. Modern thermal cameras (of less than 0.5 mega-pixel) cost an order of magnitude more than corresponding visual digital cameras of more than 10 mega-pixel (by the way, it helps a lot taking visual images at the same time as infrared images).

Bolometers and micro-bolometers

A bolometer (from Gr. *bolo*, thrown) is a thermal-radiation sensor based on the electric resistance change with temperature. The first bolometer, made by the Am. astronomer Samuel Langley in 1878, consisted of two platinum strips covered with lampblack, one strip was shielded from the radiation and one exposed to it, forming two branches of a Wheatstone bridge, using a galvanometer as indicator.

Micro-bolometers are tiny bolometers (micro-machined in a CMOS silicon wafer, see Fig. 4) used in detector arrays in modern un-cooled thermal cameras, although their response time is low. It is a grid of vanadium oxide or amorphous silicon heat sensors atop a corresponding grid of silicon. Infrared radiation from a specific range of wavelengths strikes the vanadium oxide and changes its electrical resistance.

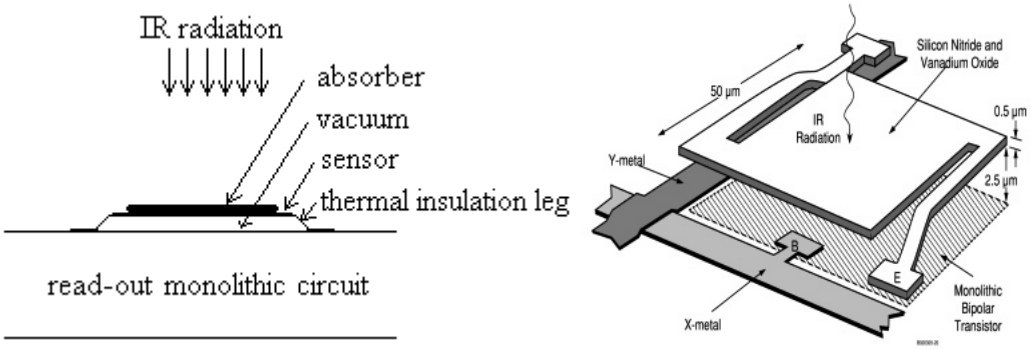

Fig. 4. Sketch of a micro-bolometer structure (and a design by Fluke-Infrared Solutions).

The word bolometric is sometimes used as synonymous of total (i.e. spectral integral), but what a bolometer detects depend on the filters used.

Pyranometers and heliometers

A pyranometer (from Gr. *pyr*, fire, *ano*, upwards), sometimes named solarimeter, is a thermopile-sensor radiometer (Fig. 5) that measures all incoming solar radiation (hemispherical, i.e. 2π stereo-radians, and total, i.e. from 0.3 μm to 3 μm in practice). It is the typical device used in meteorology and solar energy applications; it is un-powered, and typical sensitivity is 10 μV/(W/m^2).

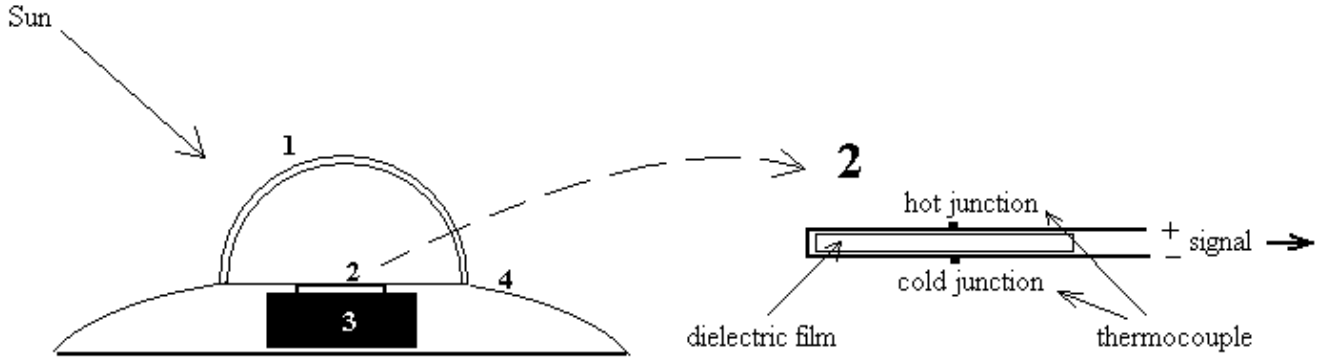

Fig. 5. Sketch of a pyranometer: 1, glass dome; 2, thermopile sensor (an array of thermocouples arranged in series and wrap around a dielectric film, as detailed in the insert); 3, thermal block; 4, radiation protector.

A pyranometer with a shadow band or shading disk blocking the direct solar beam (0.49 rad of arc), measures the hemispherical total diffuse sky radiation. Solar beam power can be deduced by difference, although another kind of instrument, the pyroheliometer, which has a narrow field of view (some 5º) is used for that purpose.

Measuring thermo-optical properties

The basic thermo-optical quantities measured at a material surface are emissivity and reflectance, and the others are computed from them.

Emissivity is measured by detecting incoming radiation from an opaque body kept at temperature *T*, under a cryogenic vacuum (to avoid reflections), and dividing the result by the corresponding Planck's equation value; either spectral or total measurements are carried out (the device is known as emissometer in either case). For total hemispherical emissivity, a simple energy balance may be used with an electrically-heated sample in a cryogenic vacuum.

Reflectance is measured by dividing the increase in irradiation detected from an opaque body (i.e. discounting emission and transmission), by a sinusoidal variation of the intended irradiation shining on the object (i.e. to discount other reflections). The device is named reflectometer, although it is also known as emissometer if an infrared source is used to shine on the object, since, for an opaque object in a narrow spectral band, Kirchhoff's law implies $\varepsilon=1-\rho$ for a given direction (several IR-bands, at several incidence angles, are measured; usually the most important bands are the atmospheric windows: 3..5 μm, and 8..12 μm). Calibration can be provided by a small specular gold sample traced to primary standards (NIST). Spectrophotometers measure either reflection or transmission.

Albedo can be measured using two opposite pyranometers aligned with solar radiation, one pointing to the Sun, and the other to the sample surface.

Absorptance in opaque bodies is computed from the energy balance $\alpha=1-\rho$, by measuring reflectance, ρ. Recall that equality between absorptance and emissivity only applies in general to the detailed balance: $\alpha_{\lambda\beta\theta T}=\varepsilon_{\lambda\beta\theta T}$. Absorptance in transparent media is measured in terms of the exiting radiation, used to compute an extinction coefficient (includes scattering). On photovoltaic cells (e.g. in solar arrays) not all the absorbed energy goes to thermal energy; for solar cells of electrical efficiency $\eta\equiv(VI)_{\max}/(EA)$, thermal absorption is $\alpha_{\text{th}}=\alpha-\eta F_{\text{p}}$, where F_{p} is the packaging factor for the cells (F_{p}=0.8..0.9 is cell area divided by panel area A), E is a standard normal irradiance (1370 W/m^2 for space cells, but 1000 W/m^2 for terrestrial cells), and $(VI)_{\max}$ the maximum electrical power delivered.

Transmittance in transparent bodies is computed in terms of the extinction coefficient and the reflectance at interfaces. Maxwell theory shows that reflectance at a dioptric interface is $\rho=(n_1-n_2)^2/(n_1+n_2)^2$; e.g. from air to glass or vice versa, $\rho=(0.33/2.33)^2=0.02$

IR windows

The spectral range of most narrow band radiation thermometers is typically determined by the optical filter. Filters are used to restrict response to selected wavelengths to meet the need of a particular application. For example, the 5±0.2 μm band is used to measure glass surface temperature because glass surface emits strongly in this region, but poorly below or immediately above this band. Next, the 3.43±0.2 μm band is often used for temperature measurement of thin films or polyethylene-type plastics etc.

Atmospheric filter. The atmospheric filter depends a lot on actual water content in the atmosphere, and aerosols content in general. Clean air has two main windows in the IR, besides the visual and radio windows (Fig. 6):

- Visible window. Incoming solar radiation energy is 95% in the λ=0.3..3 μm range (10% in the UV, 40% in the visible, and 50% in the infrared).
- Short IR window, in the range λ=3..5 μm. Complete absorption by CO_2 in the range 4.2..4.5 μm, what is used in remote sensing to detect mean air temperature in the troposphere-stratosphere. The high absorption band in 5..8 μm is used in remote sensing to measure water content in the air.
- Long IR window, in the range λ=8..14 μm. This is the main atmospheric window (see Fig. 6), being highly transparent to water vapour, carbon dioxide, smoke, and dust, although there is a small absorption band by ozone at 9.5..10 μm, what can be used to measure ozone abundance. This long-IR (or far-infrared) band is used in remote sensing to measure surface temperature from satellites. The most used material for long-IR optics is n-doped polycrystalline germanium. Since the optical refractive index of germanium is high, the reflectance from each surface is high and the net transmittance through the germanium is relatively low. The refractive index of germanium is 4.0, resulting in 36% reflectance per surface. The transmittance of uncoated germanium is only 47% through a 1 mm thick piece. In order to improve the IR transmittance of the window, a suitable antireflection coating is applied (some 2 μm thick low refracting index material like thorium fluoride, ThF), reducing window reflectance to <1%, thereby raising the transmittance to >95%. Additional coatings protect the lens from moisture.

- Radio window, in the range λ=0.01..10 m (corresponding to 30 MH..30 GHz), i.e. including the microwave range up to the Ku band.

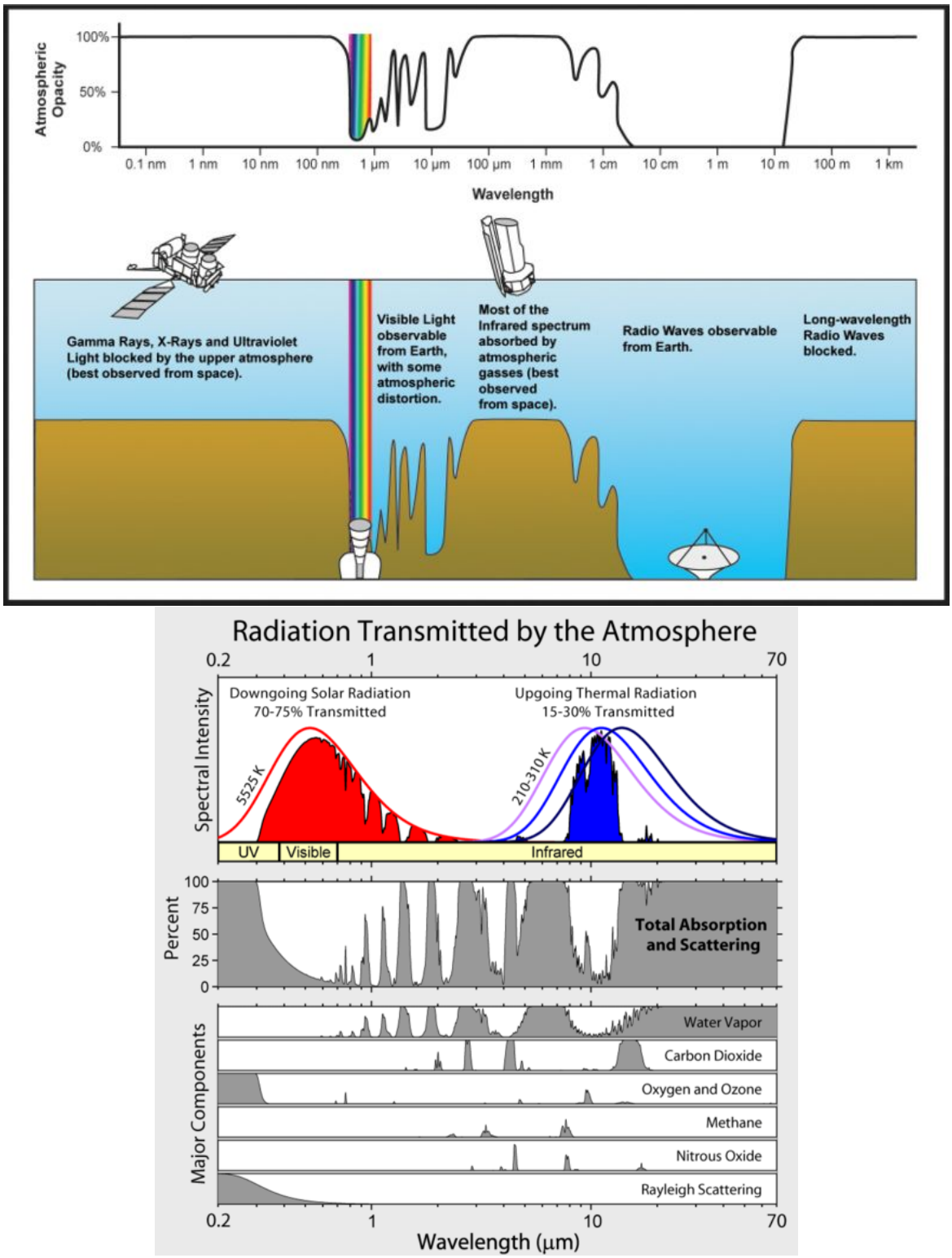

Fig. 6. The Earth's atmospheric filter (clear sky): a) general electromagnetic opacity (NASA/IPAC), and b) detailed transmittance (Wiki). The three main atmospheric windows are: the solar band (0.3..3 µm) that gives us the Sun light and heat (and allows our seeing the stars), the long infrared band (8..14 µm) that allows for some Earth cooling, and the radio band (10^{-2}..10 m, including microwaves) that allows for space radio-communications.

Earth emission energy is over 90% in the λ=3..30 μm range, with the peak around λ_{Mmax}=10 μm. To this peak in the spectrum corresponds a blackbody temperature around 300 K (in any case, close to 288 K average surface temperature). However, from the total emittance as seeing from outside, a blackbody temperature of 253 K would be deduced. A good simple model is then to take T_0=288 K as reference surface data, and deduce an average emissivity value, ε, such that $M=\varepsilon\sigma T_0^4$, what yields ε=0.60. Further spectral details of the Earth emission are (Fig. 7):

- Nearly half of Earth's emitted energy is in the long-IR atmospheric window (8..14 μm), at an apparent temperature of 288 K. Without this window, the Earth would become much too warm to support life, and possibly so warm that it would lose its water as Venus did, early in solar system history.
- Outside the long-IR atmospheric window, i.e. when the atmosphere is opaque (5..8 μm and >14 μm), emission is perceived as coming from a blackbody atmosphere at 218 K, with a total average (spectrum integral) of 258 K, what correlates well with ground measurements of sky temperature, which are $(T_{amb}-T_{sky})_{bolo}\approx$30 K and $(T_{amb}-T_{sky})_{espectral}\approx$70 K.
- Measuring the equivalent sky temperature from ground on a clear night, one gets consistent values: for total radiation, $(T_{amb}-T_{sky})_{bolo}\approx$30 K, and, in the atmospheric window $(T_{amb}-T_{sky})_{IR-window}\approx$70 K.

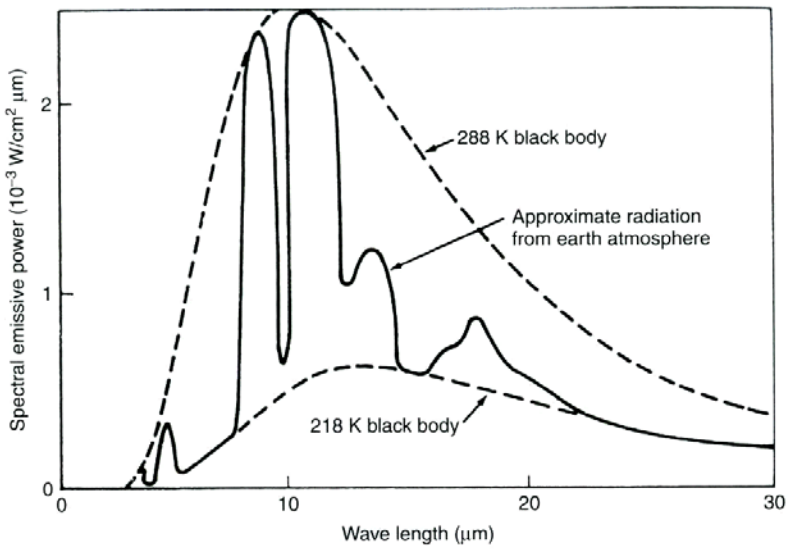

Fig. 7. The Earth's atmospheric filter for clear-sky conditions. Planet emittance as looking from outside.

When clouds are present, the visible and infrared windows disappear, leaving just the radio window, because liquid water, even in finely dispersed aerosols like in clouds, have a much higher absorption and scattering than water vapour (some 10^4 times higher in the main 8..14 μm infrared window).

Glass filter. There are several types of glass:

- Window glass (common glass, comprising >90% of all glass production), also known as soda-lime or crown glass (SiO_2 75%, Na_2O 15%, CaO 10%), is a low-melting-temperature glass used for windows and containers. Transmission has a window in 0.3<λ<2.5 μm, with a heap transmittance profile that drops from 0.9 at 0.5 μm to 0.6 at 1 μm for a 10 mm thick glass, with near-IR transmittance falling rapidly with thickness (Fig. 8). An ordinary second-surface mirror

has a solar absorptance of α=0.14 (aluminized; α=0.07 if silvered). Notice that a glass window do not let ultraviolet and infrared radiation through, what explains the green-house effect, and why filament-emission heats up bulbs of incandescent lamps (average absorptance from a 3000 K source is around 0.7).

- Quartz glass is pure silica (>99.5% SiO_2, also known as fused silica). Quartz windows (a few mm to a few cm thick) have some 90% radiation transmittance in the range $0.2<\lambda<2.5$ μm. An interesting application of selective transmission is the transparent mirror furnace, used for observing crystal growth up to 1300 K; in this furnace, a window (or the whole furnace) is made of pyrex glass (transparent in the visible) with an internal gold deposition (some 20 nm) specular in the infrared and with some transparency (τ=0.2) in the visible (pyrex is a thermal and chemical resistant glass, used for laboratory and oven work, with SiO_2 80%, B_2O_3 13%, also known as borosilicate glass).

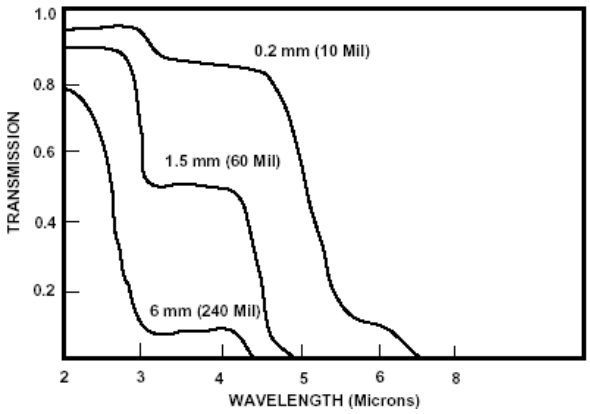

Fig. 8. Glass transmittance (lamp bulb, normal pane, thick pane).

Water filter. Water is transparent in the visible (lowest extinction coefficient is 0.02 m^{-1} at 0.55 μm, growing to 1 m^{-1} at the practical cut-offs of 0.3 μm and 0.7 μm, becoming progressively opaque in the infrared, with high absorption near 3 μm (what is used in IR heaters). Total transmission of solar radiation through 1 m of water is 35%.

Infrared windows. Table 2 presents data for some infrared transparent materials.

Table 2. IR window materials (ordered by spectral band).

Material	Formula	transmission band	Notes
Sapphire	Al_2O_3	0.15..5.5 μm	Very hard
Calcium fluoride	CaF_2	0.15.. 10 μm	Soluble
Barium fluoride	BaF_2	0.15.. 12 μm	Soluble, fragile
IR polymer	-	0.15.. 22 μm	Soft
Zinc selenide	ZnSe	0.5.. 22 μm	Soft. Transmit 99%
Germanium	Ge	1.8.. 22 μm	Hard

Thermochromic infrared shutters. Vanadium oxides change their crystalline network at a certain temperature from an IR-transparent semiconductor to a IR-opaque metal in the short IR band (3..5 μm). The most used is VO_2, which has the transition temperature around 67 ºC. The activation is performed by

pulse heating a very thin gold deposition layer (in some 15 ms), changing the transmittance from 55% to <1%.

Solar collector filter. In some applications like solar energy collectors, high absorptance with little emission is wanted, but, for a given material, high α usually implies high ε; a selective coating, however, may accomplish that, e.g. by deposition of a thin layer of a dielectric over a metal substrate, such that the coating be transparent to long wavelength (and the metal substrate is a low emitter), but opaque and absorbent at short wavelengths (e.g. SiO_2 deposition on aluminium shows an abrupt cut-off wavelength at 1.5 μm). Care should be paid to distinguish a solar shade filter, designed to prevent solar radiation to let through (as in sun glasses, snow goggles, and space suits), from a solar collector filter, whose objective is to absorb solar energy without letting long IR radiation to escape (like in a greenhouse as a whole, or in the oxide coated metal here described.

Spectral and directional modelling

The interaction of radiation and matter is difficult to model because of its inherent directional and spectral properties:

- Directionality. Rays have direction of propagation, which changes by reflection, refraction and dispersion in general. And propagation can be halted by opaque bodies.
- Spectrality. EM-radiation has a spectrum of propagating wavelengths (or frequencies, or energies), and matter is very selective to absorption-transmission-reflection-emission of different wavelengths.

As said before, the basic thermal radiation model is the blackbody, which is a body that shows no particular directional or spectral characteristics:

- Directionally, a blackbody absorbs all incident radiation independent of direction and wavelength, and emits radiation with a well-defined spectrum (only dependent on temperature) and a well-defined directionality, the cosine law for emittance, $M=M_0\cos\beta$ (β being the angle to the normal), which corresponds to a uniform radiance along any solid angle.
- Spectrally, a blackbody absorbs all incident radiation (independently of wavelength), and emits radiation in accordance with Planck's law.

Radiation heat transfer analysis is usually limited to perfectly diffusing opaque surfaces (Lambertian surfaces), for which the emerging radiance (due to own emission or reflected scattering from others) does not depends on direction (i.e. an isothermal sphere will be viewed uniformly brilliant like a frontal disc), because although the emitted power from a given area element is reduced by the cosine of the emission angle, the size of the observed area is increased by a corresponding amount.

Two-spectral-band model of opaque and diffuse surfaces (grey surfaces)

As for the spectral distribution, for most thermal problems both on ground and in space, it is good enough to consider only two types of thermal radiation, corresponding to non-overlapping regions of the spectrum, with spectral uniformity in each of the two bands: solar, and infrared (far infrared, indeed).

- Solar radiation, corresponding to a quasi-blackbody at 5800 K, which peaks in the visible range (at about 0.5 μm), and has some 10% of its energy within the ultraviolet range (0.3..0.4 μm), 40% in the visible range (0.4..0.7 μm), and 50% in the near-IR range (0.7..3 μm). For the interaction of solar radiation with matter, both for direct sunshine and for albedo, the following properties are defined:
  - Solar absorptance, α_s (usually without sub-index, since there is no possible confusion because by Kirchhoff's law it should be equal to the emissivity of a body at around 6000 K, what is of no practical interest because materials cannot withstand such high temperatures).
  - If only the solar absorptance α is given for a surface, it should be understood that the surface is opaque and that the rest of the incoming energy is diffusively reflected, i.e. $\rho=1-\alpha$. In more detailed numerical simulations (e.g. in ESARAD), four parameters are given to model the interaction of solar radiation with matter: solar absorptance α, solar transmittance τ, solar diffuse reflectance ρ_{diff}, and solar specular reflectance ρ_{spec}, such that $\alpha+\tau+\rho_{diff}+\rho_{spec}=1$. For photovoltaic materials, solar absorptance is partially converted to electricity (and the rest heats up the material). If the energy conversion efficiency is defined in terms of electrical voltage and intensity produced by incident radiation power as $\eta=(VI)_{max}/(EA)$, then the electrical power produced is $\dot{W}=\eta EA$ and the effective heating input $\dot{Q}_{in}=(\alpha-\eta)EA$.
- Infrared radiation, corresponding to a quasi-blackbody at 300 K, which peaks in the far-infrared range (at about 10 μm), and has 89% of its energy within the far-infrared range (3..30 μm). The properties averaged for this spectral band are applied to radiation emitted, absorbed, transmitted, or reflected by a given material at whatever its real temperature, from 100 K to 1000 K (a blackbody a 1000 K emits 27.3% in the near infrared range 0.7..3 μm, 72.2% in the far infrared range 3..30 μm, and 0.5% with λ>30 μm). The following properties are defined:
  - Infrared emissivity, ε_{IR} (usually without sub-index, since there is no possible confusion). Infrared absorptance is never explicitly given since, by Kirchhoff's law, it is equal to the emissivity of the body, $\alpha_{IR}=\varepsilon_{IR}$.
  - If only the infrared emissivity ε is given for a surface, it should be understood that the surface is opaque, that it absorbs infrared radiation with $\alpha_{IR}=\varepsilon$, and that the rest of the incoming energy is diffusively reflected, $\rho_{IR}=1-\alpha_{IR}$. In more detailed analysis (e.g. in ESARAD), four parameters are given to model the interaction of infrared radiation with matter: infrared emissivity ε, infrared transmittance τ, infrared diffuse reflectance ρ_{diff}, and infrared specular reflectance ρ_{spec}, such that $\varepsilon+\tau+\rho_{diff}+\rho_{spec}=1$.

When only spectral-average thermo-optical properties (one value in each band) are considered, the model is said to be of a 'grey surface'. Thermo-optical properties based on this two-band model can be found in any Heat Transfer book; vales for typical thermal control surfaces used in spacecraft thermal design are presented aside.

Even when radiation comes from intermediate-temperature sources, as red-hot materials (at 1000 K or more), the splitting of radiation effects in just the two bands described above, may be a good approximation, much simpler than taking care of all spectral details. However, for thermal radiation of very hot objects (in the range 1500..3000 K), the change with temperature of ε_{IR} must be considered, but visible radiation can still be neglected in the energy balance (only some 5% of the energy consumed in an incandescent lamp goes to visible light).

MODELLING RADIATION COUPLING

After the study of radiation properties, we deal now with the geometrical aspects involved in the radiative coupling between an emitter (a source with or without reflection from other sources) and a receiver (an absorber with or without reflection to other sources). We only consider infrared radiation coupling between opaque material surfaces separated by a non-absorbing non-scattering medium (vacuum or thin dry air, but not liquids or aerosols). Solar radiation (either direct or reflected) is considered as a known input. If non-diffuse or semi-transparent materials, or absorbing media, must be considered, then a different modelling is required (statistical ray-tracing techniques are used).

Radiation coupling for thermal control is usually studied considering lumps of material assumed to be at uniform temperature (the Lumped Network Method), following the view factor approach explained below, whereas similar radiative configurations are studied in much finer spatial detail as a further insight to thermal radiation modelling, and for illumination purposes (a detailed analysis of simple non-uniform distribution problems may help to better understand the validity of the assumptions commonly introduced in radiative heat transfer problems; e.g. the distribution of absorbed power may indicate that the isothermal assumption might be inadequate).

Radiation from a small patch to another small patch. View factors

Consider a differential surface patch dA_1, a hemisphere centred on it (Fig. 9), and a radiant power $d\Phi_1$ [W] exiting from dA_1, either because of its own emission ($d\Phi_1=dA_1\varepsilon_1\sigma T_1^4$), or due to reflection from an incident flux ($d\Phi_1=dA_1\rho_1 E_1$); no transmission from the rear of dA_1 is considered, so that in general $d\Phi_1=dA_1(\varepsilon_1\sigma T_1^4+\rho_1 E_1)$. If only IR radiation is considered, one thermo-optical parameter is needed, since $\alpha_{IR}=\varepsilon_{IR}=1-\rho_{IR}$. We want to know how much of this radiation will impinge on another infinitesimal patch dA_2 (in the hemisphere or projected on it), i.e. the irradiance E_2 [W/m^2] it gets, and how a 'viewer' at dA_2 will 'see' dA_1 (i.e. how much energy per unit time, per unit area at the source, and per unit solid angle of the optical system, will get a detector at dA_2 from dA_1).

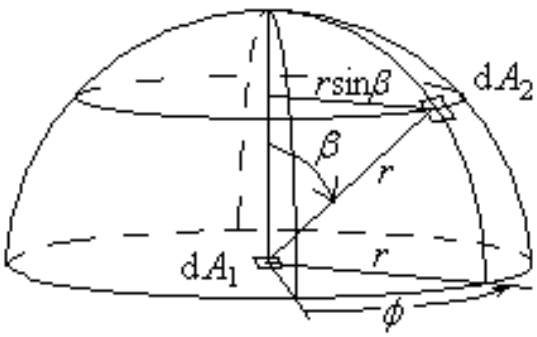

Fig. 9. Notation for studying radiation from a differential patch dA_1 to its viewing hemisphere. Let dA_2 be a surface patch at the hemisphere of radius r. Sometimes θ is used instead of β for the polar angle or co-latitude.

Perfect diffuser

Radiant power (Φ_1) and emittance (exitance, really, $M_1 \equiv d\Phi_1/dA_1 = \varepsilon_1 M_{1,bb} + \rho_{1,IR} E_1$), may be distributed along the measuring direction in a complicated way in real surfaces. We restrict our attention to perfect diffusers (diffuse surfaces in brief), for which the radiated power of a surface patch in a given direction (the intensity, $I_1 \equiv d\Phi_1/d\Omega$) varies with the cosine of the polar angle, $\cos\beta_1$, what implies that the power per projected area and solid angle (the radiance, $L_1 \equiv d^2\Phi_1/(dA_{1\perp} d\Omega)$, i.e. the 'brightness' seen by a detector), does not depends on the viewing direction, provided exitance at the surface is uniform (isothermal, with uniform emissivity, and uniformly lit and reflecting).

A blackbody is a perfect diffuser, as can be demonstrated by considering a blackbody enclosure at thermodynamic equilibrium, with a central patch dA_1 and any other patch at the hemisphere above (of area $dA_{2\perp}$); blackbody radiation being isotropic implies $d^2\Phi_{12} = d^2\Phi_{21}$ (i.e. output=input) for any direction, with $d^2\Phi_{12} = L(\beta_1) dA_{1\perp} d\Omega_{12} = L(\beta_1) dA_1 \cos\beta_1 dA_{2\perp}/r_{12}^2$, and $d^2\Phi_{21} = L(\beta_2) dA_{2\perp} d\Omega_{21} = L(0) dA_{2\perp} dA_1/r_{21}^2$; equality thence implies that $L(\beta_1) = L(0)$, i.e. the radiance of dA_1 seen from $dA_{2\perp}$ (which cannot depend on the chosen patch because of blackbody isotropy), coincides with the radiance of $dA_{2\perp}$ seen from dA_1, at any angle.

View factors

Consider two infinitesimal surface patches, dA_1 and dA_2 (Fig. 10), in arbitrary position and orientation, defined by their separation distance r_{12}, and their respective tilting relative to the line of centres, β_1 and β_2, with $0 \le \beta_1 \le \pi/2$ and $0 \le \beta_2 \le \pi/2$ (i.e. seeing each other). The radiation intercepted by surface dA_2 coming directly from a diffuse surface dA_1 will be: its radiance L_1, times its perpendicular area $dA_{1\perp}$, times the solid angle subtended by dA_2, $d\Omega_{12}$; i.e. $d^2\Phi_{12} = L_1 dA_{1\perp} d\Omega_{12} = L_1 (dA_1 \cos(\beta_1)) dA_2 \cos(\beta_2)/r^2$. The view factor, F_{12} (more explicitly written $F_{1\to 2}$) is defined as the fraction intercepted by A_2 from the total energy radiated from A_1. In the case of two infinitesimal areas, $dF_{12} \equiv d^2\Phi_{12}/(M_1 dA_1)$:

$$dF_{12} \equiv \frac{d^2\Phi_{12}}{M_1 dA_1} = \frac{L_1 d\Omega_{12} dA_1 \cos(\beta_1)}{M_1 dA_1} = \frac{\cos(\beta_1)}{\pi} d\Omega_{12} = \frac{\cos(\beta_1)}{\pi} \frac{dA_2 \cos(\beta_2)}{r_{12}^2} = \frac{\cos(\beta_1)\cos(\beta_2)}{\pi r_{12}^2} dA_2 \qquad (29)$$

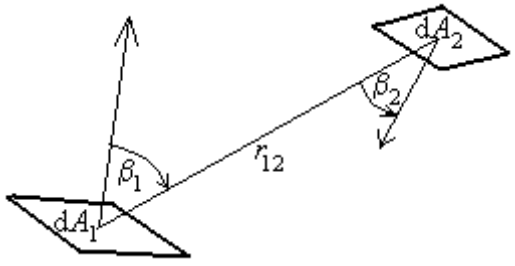

Fig. 10. Geometry and notation for view-factor definition.

whereas for finite surfaces (they must be isothermal and diffuse); the problem is just of integration (although not a trivial one):

$$\mathrm{d}F_{ij}=\frac{\cos\beta_i\cos\beta_j}{\pi r_{ij}^2}\mathrm{d}A_j \quad\Rightarrow\quad F_{ij}=\frac{1}{A_i}\int_{A_i}\left(\int_{A_j}\frac{\cos\beta_i\cos\beta_j}{\pi r_{ij}^2}\mathrm{d}A_j\right)\mathrm{d}A_i \tag{30}$$

View factor algebra

When considering all the surfaces under sight from a given one (enclosure theory), several general relations can be established among the N^2 possible view factors, what is known as view factor algebra:

- Bounding. View factors are bounded to $0\le F_{ij}\le 1$ by definition (the view factor is a fraction).
- Closeness. Summing up all view factors from a given surface in an enclosure, including the possible self-view factor for concave surfaces, must equal unity, $\sum_j F_{ij}=1$, because the same amount of radiation emitted by a surface must be absorbed at the end (no escape is possible).
- Reciprocity. Noticing from view factor definition (20) that $\mathrm{d}A_i\mathrm{d}F_{ij}=\mathrm{d}A_j\mathrm{d}F_{ji}=(\cos\beta_i\cos\beta_j/(\pi r_{ij}^2))\mathrm{d}A_i\mathrm{d}A_j$, it is deduced that $A_iF_{ij}=A_jF_{ji}$.
- Distribution. When two target surfaces are considered at once, we have $F_{i,j+k}=F_{ij}+F_{ik}$, based on area additivity in the definition.
- Composition. Based on reciprocity and distribution, when two source areas are considered together, we have $F_{i+j,k}=\left(A_iF_{ik}+A_jF_{jk}\right)\big/\left(A_i+A_j\right)$.

For an enclosure formed by N surfaces, there are N^2 view factors (each surface with all the others and itself). But only $N(N-1)/2$ of them are independent, since another $N(N-1)/2$ can be deduced from reciprocity relations, and N more by closeness relations. For instance, for a 3-surface enclosure, we can define 9 possible view factors, 3 of which must be found independently, another 3 can be obtained from $A_iF_{ij}=A_jF_{ji}$, and the remaining 3 by $\sum_j F_{ij}=1$.

Exercise 5. Find the view factor from a small area $\mathrm{d}A_1$ normal and centred with respect to a circular disc of radius R a distance H apart, from the view factor definition.

Sol.: View factor, F_{12}, is defined as the fraction of energy radiated out by A_1 that reaches A_2. For two infinitesimal patches, $\mathrm{d}F_{12}\equiv\mathrm{d}^2\Phi_{12}/(M\mathrm{d}A_1)=\cos\beta_1\cos\beta_2\mathrm{d}A_2/(\pi r_{12}^2)$. Consider the sketch in Fig. E5, representing two equivalent configurations for A_2: the said planar disc, and the projected spherical cap centred at the patch and of radius $\rho=\sqrt{H^2+R^2}$. Let $h\equiv H/R$.

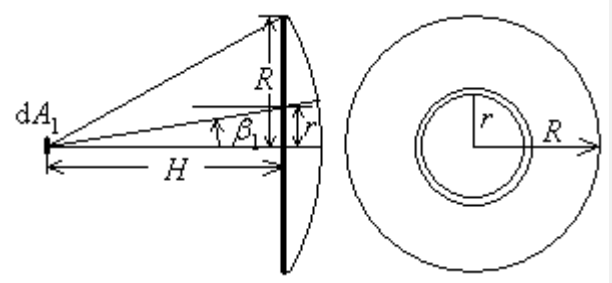

Fig. E5. Profile and front view for the two equivalent configurations to compute F_{12}: the said planar disc (in bold), and the projected spherical cap.

If we integrate $\mathrm{d}F_{12}=\cos\beta_1\cos\beta_2\mathrm{d}A_2/\left(\pi r_{12}^2\right)$ in the case of the real disc, choosing as independent variable $0\le r\le R$, and with $\cos\beta_1=\cos\beta_2=H/r_{12}$, $r_{12}=\sqrt{H^2+r^2}$, and $\mathrm{d}A_2=2\pi r\mathrm{d}r$, we have:

$$F_{12}=\int_{A_2}\frac{\cos\beta_1\cos\beta_2}{\pi r_{12}^2}\mathrm{d}A_2=\int_{r=0}^{R}\frac{\left(H/r_{12}\right)^2}{\pi r_{12}^2}2\pi r\mathrm{d}r=\int_{r=0}^{R}\frac{H^2}{\left(H^2+r^2\right)^2}\mathrm{d}\left(r^2\right)=\left[\frac{-H^2}{H^2+r^2}\right]_{r=0}^{r=R}=\frac{1}{1+h^2}$$

Of course, we might have used β_1 as independent variable to do the above integration, instead of r, but we prefer to follow another approach: to compute F_{12} by projecting the real disc area against the sphere centred in $\mathrm{d}A_1$ and bordering the disc (Fig. E5). In this case, and choosing as independent variable $0\le\beta_1\le\arctan(R/H)$, we have $\beta_2=0$ for any differential spherical patch, $r_{12}=\sqrt{H^2+R^2}$, and $\mathrm{d}A_2=2\pi r_{12}\sin\beta_1 r_{12}\mathrm{d}\beta_1$, what yields:

$$F_{12}=\int_{A_2}\frac{\cos\beta_1\cos\beta_2}{\pi r_{12}^2}\mathrm{d}A_2=\int_{\beta_1=0}^{\arctan\frac{R}{H}}\frac{\cos\beta_1}{\pi r_{12}^2}2\pi r_{12}\sin\beta_1 r_{12}\mathrm{d}\beta_1=\int_{\beta_1=0}^{\arctan\frac{R}{H}}\sin\left(2\beta_1\right)\mathrm{d}\beta_1=\left[\frac{-\cos\left(2\beta_1\right)}{2}\right]_0^{\arctan\frac{R}{H}}$$

$$=\left[\frac{1}{2}-\cos^2\beta_1\right]_0^{\arccos\frac{H}{\sqrt{H^2+R^2}}}=\frac{1}{2}-\frac{H^2}{H^2+R^2}-\left(\frac{-1}{2}\right)=\frac{1}{1+h^2}$$

Although it is a matter of choice, this second method of view-factor computation has the advantage that the radial distance is constant and the spherical patch is always normal, simplifying the integration.

The later procedure (i.e. considering the spherical cap) can be directly based on solid-angle dependence of view factors, i.e. from $\mathrm{d}F_{12}\equiv\mathrm{d}^2\Phi_{12}/(M\mathrm{d}A_1)=L_1\mathrm{d}A_1\cos\beta_1\mathrm{d}\Omega_{12}/(\pi L_1\mathrm{d}A_1)=\cos\beta_1\mathrm{d}\Omega_{12}/\pi$, and hence $F_{12}=\int\cos\beta_1\mathrm{d}\Omega_{12}/\pi=\int\cos\beta_1(2\pi\sin\beta_1\mathrm{d}\beta_1)/\pi=\int\sin(2\beta_1)\mathrm{d}\beta_1$, and so on as before. Notice that, as a function of the semi-conical angle $\alpha=\arctan(R/H)$, the view factor can also be set as $F_{12}=\sin^2\alpha$.

Finally notice that, in spite of the view factor from the patch to the disc being equal to the view factor from the patch to the spherical cap (or any surface limited by the same solid angle), the irradiance distribution is very different: it falls with $\cos^4\beta_1$ on a planar disc, and with $\cos\beta_1$ on a spherical cap. For instance, for a blackbody patch $\mathrm{d}A_1$ (say of 1 cm^2) at T_1=1000 K, with an emittance of $M_1=\sigma T_1^4$=57.8 kW/m^2 (and radiance $L_1=M_1/\pi$=18.4 kW/m^2), the irradiance on a parallel patch $\mathrm{d}A_2$ a distance d=1 m apart (say of another 1 cm^2) is $\mathrm{d}E_2=L_1\mathrm{d}A_1/d^2$=0.184 kW/m^2, deduced from the general expression, $\mathrm{d}E_2=M_1\mathrm{d}A_1F_{12}/\mathrm{d}A_2=M_1\mathrm{d}A_1\cos\beta_1\cos\beta_2/(\pi r_{12}^2)$; now, the radial variation for $\mathrm{d}A_2$ on a planar disc at a distance d is $\mathrm{d}E_2=M_1\mathrm{d}A_1\cos\beta_1\cos\beta_2/(\pi r_{12}^2)=L_1\mathrm{d}A_1\cos^2\beta/(d/\cos\beta)^2=L_1\mathrm{d}A_1\cos^4\beta/d^2$, i.e.

(184 W/m^2)·cos$^4\beta$, in our example, whereas the radial variation for dA_2 on a spherical cap with vertex at a distance d is dE_2=M_1dA_1cos$\beta_1$cosβ_2/(πr_{12}^2)=L_1dA_1cosβ/d^2, i.e. (184 W/m^2)·cosβ, in our example.

Conversely, the radiation power received by a frontal patch from any perfectly-diffuse (or blackbody) surface seen with the same solid angle in that direction, at the same temperature, is the same; i.e. we get the same irradiance from our huge spherical Sun, than from a small thumb-size circular disc at 5800 K an arm-distance away if they subtend the same solid angle (only at a small patch, like our pupil, as said).

Large compilations of view factors for different geometries exist, but not all of them admit an analytical expression. A compilation of analytical view factors may be used to solve many radiation heat transfer problems of space technology or more wide industrial interest, using the development presented below. Numerical computation of the quadruple integral implied in (30) is cumbersome; a simple procedure based on a Monte Carlo method is presented as an Example aside; among deterministic methods, one can directly compute the quadruple integral mentioned, or reduce it to a double line integral along the edges of the participating surfaces applying Stokes' theorem of vector calculus.

Before the computer era, graphical calculations were used. Nusselt, one of the pioneers in radiation heat transfer, applied the unit-sphere method to compute the view factor from a patch to any arbitrary surface; it considers the patch at the centre of a hemisphere of unit radius, the projection over the floor (where the patch sits) of the layout of the solid angle subtended by the arbitrary surface over the unit hemisphere, has an area equal that coincides with the view factor.

Radiative coupling

We want to find the heat transfer by radiation from a surface within evacuated enclosures formed by opaque Lambertian (i.e. perfectly diffuse) grey surfaces, each considered isothermal (i.e. a lumped radiation network). The meaning of terms:

- Surface radiation in vacuum means that we only consider surfaces as the source and sink of radiation, with no participating media in between. This may be a good approximation to radiation through air (particularly through dry air within not too-large-size systems).
- Enclosure means that all the 2π-steradians of viewing from a surface patch are considered. A background surface can always be thought to close an otherwise open environment (in space, the cosmic background, with T_∞=2.7 K).
- Opaque means that no transmission of radiation through the surface is considered (for semitransparent materials, a Monte Carlo ray-tracing attenuation model should be applied).
- Lambertian means that surfaces are considered perfectly diffuse for emission and for reflection. Non-diffuse inputs (directional beams like solar radiation and lasers) must be accounted aside as ‘heat gains’. Non-diffuse outputs like mirror reflections must be accounted separately. The Monte Carlo model of ray tracing can accommodate any non-Lambertian behaviour.

- Grey surface means that all thermo-optical properties are independent of wavelength in the far IR band, which is the only one being accounted in the network model.

Lumped network method (LNM)

In the lumped network method (LNM), the enclosure is divided into *N* isothermal surfaces (sides); each surface, of area A_i and temperature T_i, is considered a thermodynamic closed subsystem with energy balance $C_\mathrm{i}\,\mathrm{d}T_\mathrm{i}/\mathrm{d}t = \dot{W}_\mathrm{i,dis} + \dot{Q}_\mathrm{i}$, where C_i is the node thermal capacity, T_i its temperature, $\dot{W}_\mathrm{i,dis}$ a possible dissipative work power (from Joule effect, or collimated beams), and $\dot{Q}_\mathrm{i}$ the net heat rate received (always due to temperature difference) which we split in its conductive (contact) and radiative (non-contact) parts, $\dot{Q}_{i,\mathrm{con}}$ and $\dot{Q}_{i,\mathrm{rad}}$, respectively (we use 'con' on purpose, to add convection, if any, to the conduction term). When a material element has several faces (e.g. a plate with two sides), it may be advantageous to consider each face as a different node, with a proper share of the total thermal capacity (e.g. for a plate, instead of one whole node with two heat-radiation inputs, one may assign two nodes each with just one heat-radiation input, and an internal heat-conduction coupling that can be approximate or just a high-enough value to force the same temperature for the two half-plates).

Radiation heat rates are obtained in terms of exitances M_j at each surface *i*, in the following way. At a surface A_j, if there is any radiation heat-rate, $\dot{Q}_{i,\mathrm{rad}}$, it must be equal to the net radiation input, $\dot{Q}_{i,\mathrm{rad}} = \Phi_{i,\mathrm{in}} - \Phi_{i,\mathrm{out}}$ (input radiation power minus output), which can be set in these different forms:

- Choosing the system interface a little bit inside the surface (when absorption and reflection of incoming radiation, have already taken place), net heat input equals absorption minus emission:

$$\dot{Q}_{i,\mathrm{rad}} = A_i\left(\alpha_i E_i - \varepsilon_i M_{i,\mathrm{bb}}\right) \tag{31}$$

- Choosing the system interface a little bit outside the surface (when absorption and reflection of incoming radiation, have not yet taken place), net heat input equals irradiance minus exitance (times the area):

$$\dot{Q}_{i,\mathrm{rad}} = A_i\left(E_i - M_i\right) \tag{32}$$

- Eliminating the irradiance from equations (31) and (32):

$$\dot{Q}_{i,\mathrm{rad}} = \frac{M_i - M_{i,\mathrm{bb}}}{\dfrac{1-\varepsilon_i}{A_i\varepsilon_i}} \tag{33}$$

  which may be interpreted from an electrical analogy as 'a flow $\dot{Q}_{i,\mathrm{rad}}$ directly proportional to a force-difference, M_i–$M_\mathrm{i,bb}$, and inversely proportional to a resistance of value $(1-\varepsilon_i)/(A_i\varepsilon_i)$'. It is cumbersome to extrapolate equation (33) to the blackbody limit, since both, $1-\varepsilon_i$ and M_i–$M_\mathrm{i,bb}$, tend to zero, but the blackbody case is much simpler, as explained below.

Let consider now the interaction among surfaces. The net radiation heat received by surface *i* from surface *j* is $\dot{Q}_{i\leftarrow j} = \Phi_{j\to i} - \Phi_{i\to j}$, where we keep to the tradition of naming $\dot{Q}_{i\leftarrow j}$ (shortly $\dot{Q}_{ij}$) the 'heat

from *j* to *i*', as a shorthand for 'the net radiation flux received by surface *i* from surface *j*'; notice however, that with this naming, it can happen that $\dot{Q}_{i\leftarrow j}\neq 0$ with $T_i=T_j$, contrary to the definition of heat as energy flow by temperature difference). From all the enclosure:

$$\dot{Q}_{i,\mathrm{rad}}=\sum_j \dot{Q}_{ij}=\sum_j\left(\Phi_{j\to i}-\Phi_{i\to j}\right)=\sum_j\left(M_j A_j F_{ji}-M_i A_i F_{ij}\right)=\sum_j\left(M_j A_i F_{ij}-M_i A_i F_{ij}\right)=\sum_j \frac{M_j-M_i}{\frac{1}{A_i F_{ij}}} \qquad (34)$$

where radiative fluxes (Φ) have been put in terms of exitances (M) and view factors (F_{ij}), $\Phi_{i\to j}=M_i A_i F_{ij}$), and the reciprocity relation applied: $A_i F_{ij}=A_j F_{ji}$. Another way to get equation (34) is: $\dot{Q}_{i,\mathrm{rad}}=A_i\left(E_i-M_i\right)=\sum_j A_j F_{ji} M_j-A_i M_i=\sum_j A_i F_{ij} M_j-A_i M_i\sum_j F_{ij}=\sum_j A_i F_{ij}\left(M_j-M_i\right)$.

The equations to solve to get the intermediate variables M_i (and finally the $\dot{Q}_{i,\mathrm{rad}}$ and T_i) are the energy balance at every node, $dH_i/\mathrm{d}t=\dot{W}_{i,\mathrm{dis}}+\dot{Q}_{i,\mathrm{con}}+\dot{Q}_{i,\mathrm{rad}}$, where $\mathrm{d}H_i=m_i c_i \mathrm{d}T_i/\mathrm{d}t$ is the enthalpy change rate (equal to the internal energy change rate, $\mathrm{d}E_i$, in incompressible systems), and the network system can be cast as:

$$\dot{Q}_{i,\mathrm{rad}}=\frac{M_i-M_{i,\mathrm{bb}}}{\frac{1-\varepsilon_i}{A_i\varepsilon_i}}=\sum_j \frac{M_j-M_i}{\frac{1}{A_i F_{ij}}}=\frac{dE_i}{\mathrm{d}t}-\dot{Q}_{i,\mathrm{con}}-\dot{W}_{i,\mathrm{dis}} \qquad (35)$$

representing three sets of equations (one per each equal sign) to be solved for the three sets of unknowns considered: $\dot{Q}_{i,\mathrm{rad}}$, M_i, and $M_{i,\mathrm{bb}}$ (or T_i, since $M_{i,\mathrm{bb}}=\sigma T_i^4$), and all the other parameters are assumed known (areas, emissivities, view factors, and the last three terms in (35) as a function of temperatures).

In the case of blackbody surfaces, Eq. (35) reduces to:

$$\dot{Q}_{i,\mathrm{rad}}=\sum_j A_i F_{ij}\sigma\left(T_j^4-T_i^4\right)=\frac{dH_i}{\mathrm{d}t}-\dot{Q}_{i,\mathrm{con}}-\dot{W}_{i,\mathrm{dis}} \qquad (36)$$

allowing a simple interpretation of the radiative coupling ($\dot{Q}_{ij}=\sigma R_{ij}\left(T_j^4-T_i^4\right)$) as $R_{ij}=A_i F_{ij}$. Notice that one set of equations and unknown have disappeared from (35) to (36), since for $\varepsilon_i=1$ it is $M_i=M_{i,\mathrm{bb}}$. Remember that, although $\dot{Q}_{ij}\equiv A_i F_{ij}\left(M_j-M_i\right)$ is termed 'heat from *j* to *i*', it is not properly heat but net radiation exchange.

Another case that admits a simple analytical solution is the heat exchange between two isothermal diffuse surfaces (1 and 2) that form an enclosure. The heat flow from surface 1 to surface 2 in general, $\dot{Q}_{21}$ (often written as $\dot{Q}_{12}$ because the sign is obvious), and the radiative coupling R_{12} (such that $\dot{Q}_{12}=\sigma R_{12}\left(T_2^4-T_1^4\right)$, do not confuse it with the thermal resistance, defined by $\dot{Q}_{12}=\left(T_2-T_1\right)/R_{12}$), are:

$$\dot{Q}_{21}=-\dot{Q}_{12}=\frac{\sigma T_1^4-\sigma T_2^4}{\frac{1-\varepsilon_1}{\varepsilon_1 A_1}+\frac{1}{A_1 F_{12}}+\frac{1-\varepsilon_2}{\varepsilon_2 A_2}} \quad\rightarrow\quad R_{12}=\frac{1}{\frac{1-\varepsilon_1}{\varepsilon_1 A_1}+\frac{1}{A_1 F_{12}}+\frac{1-\varepsilon_2}{\varepsilon_2 A_2}} \qquad (37)$$

and, in the particular case where surface 1 is convex at all points, i.e. a convex closed body within a container (i.e. F_{12}=1), (37) simplifies to:

$$\dot{Q}_{21}=\frac{\varepsilon_1 A_1\sigma\left(T_1^4-T_2^4\right)}{1+\frac{A_1\varepsilon_1}{A_2\varepsilon_2}\left(1-\varepsilon_2\right)} \quad\rightarrow\quad R_{12}=\frac{\varepsilon_1 A_1}{1+\frac{A_1\varepsilon_1}{A_2\varepsilon_2}\left(1-\varepsilon_2\right)} \tag{38}$$

When the enclosure is large (A_1<<A_2), the heat exchanged by radiation, $\dot{Q}_{12}=\varepsilon_1 A_1\sigma\left(T_2^4-T_1^4\right)$, and radiative coupling, $R_{12}=\varepsilon_1 A_1$, become independent of the thermo-optical properties of the enclosure (assumed opaque, of course), and the radiation inside the cavity tends to blackbody radiation independently of geometry and properties. This simplest configuration was considered when first presenting radiation heat transfer in (3).

Exercise 6. Consider a hemispherical shell of 1 m in diameter, at 500 K, a circular disc of 0.1 m in diameter, concentric, in the base plane and at 300 K, and the circular corona at the base that completes the closure of the hemisphere, also at 500 K. Assume that there is only heat transfer by radiation (no convection and no conduction through the contacts). Find the heat transfer received by the disc in the following cases:

a) Assuming that all surfaces are blackbodies.

b) Assuming that all surfaces are grey-bodies with ε=0.8.

Sol.: The sketch and notation is presented in Fig. E6.

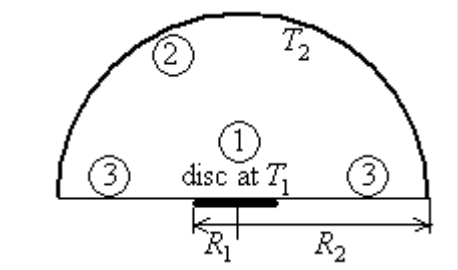

Fig. E6. Disc radiatively heated by a hemispherical dome.

a) Assuming that all surfaces are blackbodies.

In this case that there are no reflections, the disc only sees the dome, and the heat received by 1 is $\dot{Q}_{12}=A_2F_{21}\sigma\left(T_2^4-T_1^4\right)$; using the reciprocity relation A_2F_{21}=A_1F_{12} simplifies the problem, since F_{12}=1 because all the energy radiated by surface 1 falls on surface 2. It follows then $\dot{Q}_{12}=A_1F_{12}\sigma\left(T_2^4-T_1^4\right)=\left(\pi D_1^2/4\right)\sigma\left(T_2^4-T_1^4\right)$=($\pi$0.1^2/4)·5.67·10^{-8}·(500^4–300^4)=24 W. Notice that the heating of the disc does not depend on the temperature of the corona 3 (neither on its thermo-optical properties), if surface 2 is a blackbody at a fixed temperature (but the state of 3 would have an influence on the energy balance of 2).

b) Assuming that all surfaces are grey-bodies with ε=0.8.

In this case we have a two-surface enclosure (the disc 1 of area πD_1^2/4, and the rest 2 plus 3 of area πD_2^2+π(D_2^2–D_1^2)/4), with $F_{1,2+3}$=1, obtaining for $\dot{Q}_{2+3,1}=-\dot{Q}_{1,2+3}$:

$$\dot{Q}_{1,2+3}=\frac{A_1\sigma\left(T_2^4-T_1^4\right)}{\frac{1}{\varepsilon_1}+\frac{A_1}{A_{2+3}}\left(\frac{1}{\varepsilon_2}-1\right)}=\frac{\left(\pi D_1^2/4\right)\sigma\left(T_2^4-T_1^4\right)}{\frac{1}{\varepsilon}+\frac{\pi D_1^2/4}{\pi D_2^2+\pi\left(D_2^2-D_1^2\right)/4}\left(\frac{1}{\varepsilon}-1\right)}=\frac{\left(\pi D_1^2/4\right)\varepsilon\sigma\left(T_2^4-T_1^4\right)}{1+\frac{D_1^2}{5D_2^2-D_1^2}(1-\varepsilon)}=$$

$$=\frac{\pi\left(0.1^2/4\right)(0.8)\left(5.67\cdot10^{-8}\right)\left(500^4-300^4\right)}{1+\frac{0.1^2}{5\cdot1^2-0.1^2}(1-0.8)}\approx\pi\frac{0.1^2}{4}0.8\cdot5.67\cdot10^{-8}\left(500^4-300^4\right)=19\text{ W}$$

i.e. the disc receives 19 W from the rest (the hemisphere and the corona). Notice that, in this case of small receiving area, the solution is quasi-linearly proportional to ε_1, and independent of the particular geometry of the enclosure.

Radiation distribution in simple geometries

The view factor approach used above to compute radiative couplings between isothermal diffuse surfaces, only yields global radiant flows, but do not show how the radiation flux distributes on a given surface. One might refine the thermal network model, using small isothermal patches, to find a discrete distribution of radiant fluxes, but what we present now is some analytical solutions for these radiation fields, which may serve to check numerical lumped network codes, or to allow a more sound choice of nodes in a practical network, or to gain an insight in radiometry (and photometry).

Radiation from a point source to a large plate

Consider the case of a planar surface being irradiated from a point power source (Fig. 11) at a distance H and strength Φ_1 (in watts for total radiation, or in lumens for visual radiation; by the way, this is basic for the design of artificial light-appliance distribution). The point source has an isotropic intensity $I_1=\Phi_1/(4\pi)$ (in W/sr for total radiation, or in lm/sr=cd for visual radiation), and a differential patch, $\mathrm{d}A_2$, on the plane, at a distance R from the sub-source point (a distance $d_{12}=\sqrt{H^2+R^2}$ to the source); the radiation falling on $\mathrm{d}A_2$ is $\mathrm{d}\Phi_{12}=I_1\mathrm{d}\Omega_{12}$, where $\mathrm{d}\Omega_{12}$ is the solid angle subtended by $\mathrm{d}A_2$ from the source, namely $\mathrm{d}\Omega_{12}=\mathrm{d}A_{2\perp}/d_{12}^2=\mathrm{d}A_2\cos(\beta_2)/d_{12}^2$, β_2 being the angle between the viewing direction and the perpendicular to the plane; finally, the radiation per unit area, E_2 (irradiance, in W/m^2, for total radiation, or illuminance, in lm/m^2=lx, for visual radiation), is $E_2=\mathrm{d}\Phi_{12}/\mathrm{d}A_2=(\Phi_1/(4\pi))H/(H^2+R^2)^3=(\Phi_1/(4\pi H^2))\cos^3(\beta_2)$, the famous cosine-cube law of illumination, represented in Fig. 11. It can be checked that the whole plane gets half of the source power, i.e. $\int_0^\infty E_2\cdot2\pi R\mathrm{d}R=\Phi_1/2$.

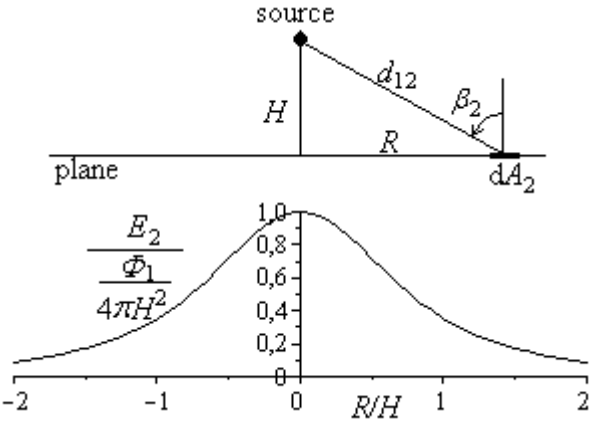

Fig. 11. Geometric sketch and irradiance distribution, $E_2(R)$, on a plane due to an isotropic point source of power Φ_1 at a distance H.

Radiation from a small patch to a large plate

Consider the radiation from a small source of area dA_1 to a planar surface problem. The difference with the point-source problem is that radiation from the source patch is not isotropic in the 4π steradians, but goes as $\cos\beta_1$ in the hemisphere facing dA_1. If the emitting patch is parallel to the plane, at a distance H, and emits a power $d\Phi_1=M_1 dA_1$ diffusively (e.g. as a blackbody , of emittance $M_1=\sigma T_1^4$), the radiation intensity in the direction β_1 is $dI_1=(M_1/\pi)dA_{1\perp}=(M_1/\pi)dA_1\cos(\beta_1)$ (it would be uniform if per unit projected area in that direction), and the irradiation on the plane $dE_2=dI_1\cos\beta_2/d_{12}^2=(M_1 dA_1/(\pi H^2)\cos^4(\beta_1)$, since $\beta_2=\beta_1=\arccos(H/d_{12})$ in this case. Notice that this is a cosine-to-the-fourth law, instead of the cosine-cube for the point source. It can be checked that now the full radiated energy impinges on the plane, $\int_0^\infty dE_2 \cdot 2\pi R dR = d\Phi_1$, instead of the half, for the point source case.

If the emitting patch is not parallel to the plane, but tilted an angle β so that the normal to the patch intersects the plane at the point $(x_n,0)$ in the plane coordinates (x,y) centred at the sub-patch point $(\tan(\beta)=x_n/H)$, then the distance from the patch to a generic point is $d_{12}=(H^2+x^2+y^2)^{1/2}$, the distance from the patch to the point $(x_n,0)$ is $d_0=(H^2+x_n^2)^{1/2}$, and the distance between the two points $r_n=((x-x_n)^2+y^2)^{1/2}$. The angular departure of a point (x,y) to the normal direction from the patch, β_1, is given by the cosine law of triangles, $\cos\beta_1=(d_{12}^2+d_0^2-r_n^2)/(2d_{12}d_0)$. The radiation intensity in the direction β_1 is again $dI_1=(M_1/\pi)dA_1\cos\beta_1$, and the irradiation at a generic point on the plane $dE_2=dI_1\cos\beta_2/d_{12}^2=(M_1 dA_1 H\cos\beta_1/\pi)/d_{12}^3$, since $\cos\beta_2=H/d_{12}$. Substitution yields the explicit form:

$$dE_2 = \frac{HM_1 dA_1}{\pi\sqrt{H^2+x_n^2}} \frac{H^2+xx_n}{\left(H^2+x^2+y^2\right)^2} \qquad (39)$$

which is represented in Fig. 12 for the case $x_n=H$ (45º tilting of the patch), and the reference case $x_n=0$ (which corresponds to the parallel-patch case, solved before). A contour map of irradiance levels on the plane (x,y) is shown, to point out the fact that it is no longer axi-symmetric. Notice that the maximum irradiance is in between the closest point (the sub-patch point, $x=0$) and the perpendicular point (the intersection with the normal to the patch, $x=x_n$). Finally notice that the source patch only shines on the semi-plane $x>-H^2/x_n$ (the other half, $x<-H^2/x_n$, would be irradiated by the rear side of the patch.

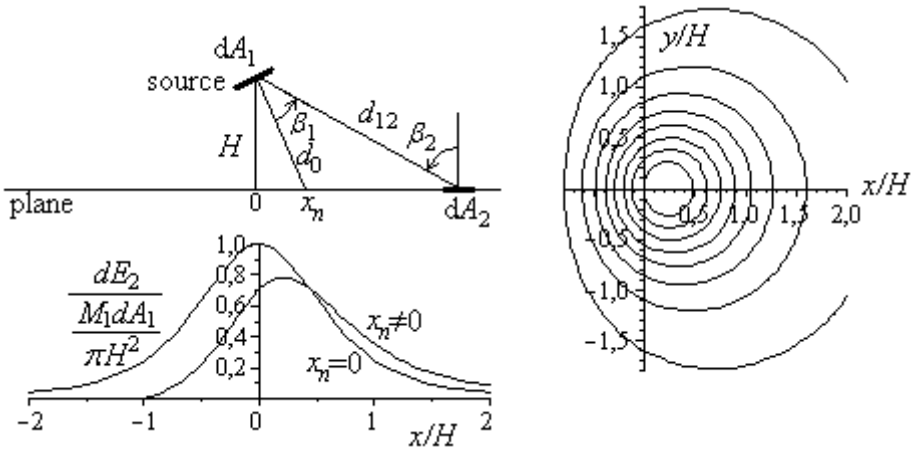

Fig. 12. Geometric sketch, and irradiance distribution on a plane, E_2, due to a small radiation patch dA_1 of emittance M_1 at a distance H; a contour plot for the latter is plotted for the case $x_n=H$ (45º tilted patch), and a profile of the irradiances at the line $y=0$ for both $x_n=H$ (45º tilted patch) and .$x_n=0$ (parallel patch).

Let us now consider the radiation from an infinite planar surface to a small tilted patch of area dA_1, with $\tan(\beta)=x_n/H$ as before. The distance from a generic point (x,y) to the patch is $d_{12}=(H^2+x^2+y^2)^{1/2}$, as before, and the same for the distance from the point to the patch, $d_0=(H^2+x_n^2)^{1/2}$, the distance between the generic point and the normal point, $r_n=((x-x_n)^2+y^2)^{1/2}$, and the angular departure of a point (x,y) to the normal direction from the patch, $\cos\beta_1=(d_{12}^2+d_0^2-r_n^2)/(2d_{12}d_0)$. The radiation intensity emitted by dA_2=dxdy in the direction β_2 is d$I_2=(M_2/\pi)$d$A_2\cos\beta_2$, and its contribution to the irradiation at the patch dA_1 is dE_1=d$I_2\cos\beta_1/d_{12}^2=(M_2dA_2H\cos\beta_2/\pi)/d_{12}^3$, since $\cos\beta_1=H/d_{12}$. Substitution yields the explicit form:

$$\mathrm{d}^2E_1=\frac{HM_2\mathrm{d}x\mathrm{d}y}{\pi\sqrt{H^2+x_n^2}}\frac{H^2+xx_n}{\left(H^2+x^2+y^2\right)^2} \tag{40}$$

which is the same as (39) but with subindices 1 and 2 exchanged, because the second-order differential used here is just an artifice to match differentials, since dxd$y\equiv$dA_2. This equivalence means that the irradiation E on a given small patch (1), due to the emittance M of another fixed small patch (2), is the same whichever is considered the source, provided both radiate diffusively.

If we know the emittance at every point in the plane, $M_2(x,y)$, integration of (40) would gives us the total irradiance on dA_1 due to a planar distribution of sources. The simplest case is when the plane has uniform emittance (i.e. an isothermal plane), in which case, performing the integration (the change $y=\sqrt{1+x^2}\tan(\phi)$ makes it easier) yields the result:

$$E_1=\int_{x=x_m}^{\infty}\mathrm{d}x\int_{-\infty}^{\infty}\frac{HM_2}{\pi\sqrt{H^2+x_n^2}}\frac{H^2+xx_n}{\left(H^2+x^2+y^2\right)^2}\mathrm{d}y=M_2\frac{1+\dfrac{H}{\sqrt{H^2+x_n^2}}}{2}=M_2\frac{1+\cos(\beta)}{2} \tag{41}$$

The view factor from the plane (recall that it must be isothermal) to the patch, is the power received on the patch, E_1dA_1, divided by the power emitted by the plane, M_2A_2, i.e. d$F_{21}\equiv E_1$dA_1/M_2A_2, which tends to zero for an infinite plate; but the view factor from the tilted patch to the infinite plate, F_{12}, is finite, and

can be calculated from the previous one by the reciprocity relation, $dA_1F_{12}=A_2dF_{21}$ (see the view factor algebra and a compilation of analytical solutions, aside), to yield $F_{12}=E_1/M_2=(1+\cos(\beta))/2$. Of course, this view factor can be computed directly from the definition, $F_{12}=\int(\cos(\beta_1)\cos(\beta_2))dA_2/(\pi r^2)$, with β_1 being the angular position of a patch in 2 from the normal to patch 1, computed by the cosine-rule as $\cos(\beta_1)=(r_0^2+r^2-d_0^2)(2rr_0)$, with $r_0 \equiv \sqrt{1+\tan^2(\beta)}$ being the distance from patch 1 to the normal intersecting point in the plane (in units of patch-plane separation), $r \equiv \sqrt{1+x^2+y^2}$ being the distance from patch 1 to patch 2 (in units of patch-plane separation), and $d_0 \equiv \sqrt{x^2+\left(y-\tan(\beta)\right)^2}$ being the distance from patch 3 to the normal intersecting point of patch 1 in the plane (in units of patch-plane separation); $\cos(\beta_2)=1/r$ is built from the angular position of patch 1 from the normal to patch 2, and $dA_2=dxdy$; namely:

$$F_{12}=\int_{\frac{-1}{\tan(\beta)}}^{\infty}\int_{-\infty}^{\infty}\frac{\cos(\beta_1)\cos(\beta_2)}{\pi r^2}dxdy \quad \text{with} \begin{cases} \cos\beta_1=\dfrac{r_0^2+r^2-d_0^2}{2rr_0}, & r_0\equiv\sqrt{1+\tan^2(\beta)} \\ & r\equiv\sqrt{1+x^2+y^2} \\ \cos\beta_2=\dfrac{1}{r}, & d_0\equiv\sqrt{x^2+\left(y-\tan(\beta)\right)^2} \end{cases} \quad (42)$$

$$F_{12}=\int_{\frac{-1}{\tan(\beta)}}^{\infty}\frac{\cos(\beta)+y\sin(\beta)}{2\left(1+y^2\right)^{3/2}}dy=\frac{1+\cos(\beta)}{2}$$

Radiation from a point source to a sphere, and how it is seen

Consider the case of a sphere of radius R being irradiated from a point source of radiant power Φ_1 at a distance H. The point source has an isotropic intensity $I_1=\Phi_1/(4\pi)$, and a differential patch on the sphere, $d^2A_2=R\sin(\theta)d\theta d\phi$, at a distance $R\sin(\theta)$ from the axis (a distance $d_{12}=\sqrt{\left(H+R\left(1-\cos(\theta)\right)\right)^2+R^2\sin^2(\theta)}$ to the source); the radiation falling on d^2A_2 is $d^2\Phi_{12}=I_1d^2\Omega_{12}$, where $d^2\Omega_{12}$ is the solid angle subtended by d^2A_2 from the source, namely $d^2\Omega_{12}=d^2A_{2\perp}/d_{12}^2=dA_2^2\cos\beta_2/d_{12}^2$, β_2 being the angle between the viewing direction and the perpendicular to the sphere, given by the cosine law of triangles, $\cos(\pi-\beta_2)=(d_{12}^2+R^2-(R+H)^2)/(2Rd_{12})$; finally, the radiation per unit area is $E_2=d^2\Phi_{12}/d^2A_2=(\Phi_1/(4\pi))\cos(\beta_2)/d_{12}^2$; when $E_2(\theta)$ is plotted for given data (R,H), a bell-shape irradiance distribution is obtained, with a maximum at the closest point, $E_2(0)=(\Phi_1/(4\pi))/H^2$, falling to zero axisymmetrically at the tangential point of central angular position $\theta_t=\arccos(R/(R+H))$, and nil on the sphere shadow.

The case of a long-distance point source is of much interest (think on the Earth or the Moon irradiated by the Sun). When $H>>R$, the collimated beam shines on half of the sphere ($\theta_t=\pi/2$), with a surface irradiance proportional to $\cos\theta$ (irradiance normal to the beam is uniform, $E=\Phi/(4\pi d^2)$). But this is how the sphere gets radiant energy (i.e. is 'illuminated'); to know how the sphere releases radiant energy is more complicated. If the sphere was a blackbody, it would absorb all incoming radiation, adjusting its temperature field until emission globally matches the energy balance, but the details of the temperature field depend on thermal conductivity and dynamics (if the sphere is spinning); e.g., if the Moon was a blackbody, it would not show phases (it would not reflect sunrays and would always show black to our eyes, in a black background, i.e. invisible except for star occultation), but we might see it with a thermal camera as a bright disc over the black background, with the thermal bright slightly decreasing from the

centre to the rim if the Moon were not perfectly conductive to be isothermal, which is not the case, of course. But the Moon is neither a blackbody, and it partially reflects solar input in the solar spectral band (0.3..3 μm) besides emitting in the infrared (3..30 μm) because of its surface temperature field.

Let us start by looking at the sphere precisely along the beam direction. If the sphere was a Lambertian diffuser (the Moon is not), we would see with our eyes a lit disc darker at the limb (the rim), like in Fig. 13a. If we looked with a thermal camera, we would see a similar bright disc, darker at the rim too in the normal case of non-infinite conductivity and thus non-isothermal surface. Perhaps this result is best understood with a tilted plane instead of the spherical geometry; it is clear that a light beam will heat up more a normal planar plate than if it were tilted an angle θ, because a given surface area-patch will get a smaller normal irradiance if tilted ($E=E_0\cos\theta$); consequently, the fraction of that irradiance reflected by that patch will also be smaller, a total of $\rho E=\rho E_0\cos\theta$ [W/m^2] if ρ is the surface reflectance, with a directional intensity distribution following the cosine law if perfectly diffuse, i.e. proportional to the cosine of the zenith angle ($\cos\beta$), and, although the radiance or apparent brightness from any viewing direction would be the same because it refers to normal area in the viewing direction ($dA/\cos\beta$), the original shortage of impinging radiation ($E_0\cos\theta$) remains.

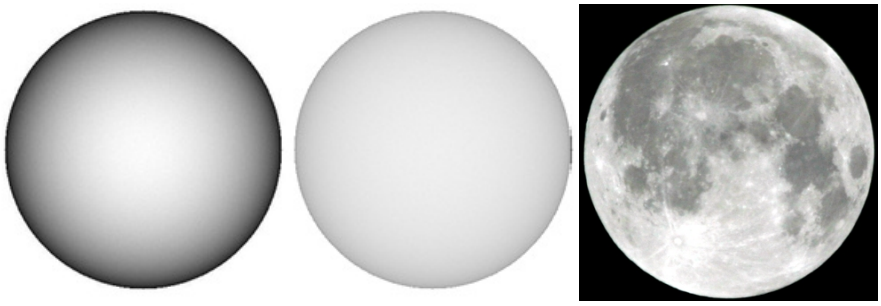

Fig. 13. a) Reflection of uniform parallel light on a perfect spherical diffuser (polished but Lambertian, not specular). b) Reflection on a real rough-surface sphere (with some retro-reflection at the rim). Not to be confused with own emission from an isothermal sphere, which would be seen (with a thermal camera for T<1000 K) nearly uniformly bright if Lambertian. c) Full moon reflectance (deep retro-reflection).

By the way, we have seen that a perfect spherical diffuser (Fig 13a) is seen darker at the periphery (a planar perfect diffuser will be uniformly bright whatever its inclination). A perfect emitter at a given temperature, whatever its geometry, will look uniformly bright because the cosine-law of emission compensates with the area projection. Hence, if the Sun were a perfect emitter, it will be seen uniformly bright; but it happens that the Sun is not Lambertian and it is darker near the limb.

Going on with reflexions, if we look at a different phase angle (the angle between the Sun-Moon and Moon-Observer lines; let follow with the Moon as our object sphere), we see that only a part of a disc is visible to our eyes (in plane geometry, a lune or crescent is a concave-convex area bounded by two arcs, a semicircle and a semi-ellipse in our case, whereas a convex-convex area is called a lens). The brightness in the crescent is maximum at the subsolar point (or at the closest rim point, if the subsolar point lies at the back), and decreases to zero at the terminator (the line separating the illuminated and dark part). Well, some brightness can be observed on the dark side of the Moon, corresponding to the second reflection of

Sun rays first reflected by the Earth, i.e. the earthshine. When looking at a crescent Moon with a thermal camera (i.e. in the far infrared band), you see the full circle bright, a little brighter towards the Sun due to its higher temperature. Notice that the Moon (and all planets and moons with regolith material) do not show retro-reflection effect in the infrared because reflection in the far infrared is negligible ($1-\varepsilon=1-0.94=6\%$ of the infrared exitance), but there are directional effects on the Moon infrared emission that produce a similar effect.

Considering again the Moon at full moon phase, and noticing that Moon spins almost 30 times slower than the Earth, one may neglect thermal inertia as a first approximation and compute surface temperature distribution based on the local energy balance at a patch tilted an angle θ to the normal (i.e. located at a central angle θ in the Moon), $\alpha E\cos\theta=\varepsilon\sigma T^4$, which, with a frontal albedo $\rho=0.10$ and emissivity $\varepsilon=0.94$ yields a temperature distribution $T=(\alpha E\cos\theta/(\varepsilon\sigma))^{1/4}=((1-0.1)\cdot 1370\cdot\cos\theta/(0.94\cdot 5.67\cdot 10^{-8}))^{1/4}=390(\cos\theta)^{1/4}$ K, i.e. 390 K at the centre (the subsolar point), 358 K at $\theta=45^o$ (i.e. 71% off-centre) and 0 K at the rim ($\theta=0$); real values are 397 K, 374 K, and around 300 K, respectively, so that the model is not bad, except close to the rim, and on the back side, of course, where real surface temperatures quickly fall from some 300 K at the limb to 100 K at subsolar opposition (this 'high' value is due to the effect of thermal conductivity and thermal capacity (the Moon is spinning; that is why the minimum temperatures, down to 20 K in a permanently shadowed crater, are found at the Poles).

Radiation from a small patch to a sphere

When a central facing patch is considered instead of the point source, the result is similar: $\mathrm{d}\Phi_1=M_1\mathrm{d}A_1$, $\mathrm{d}I_1=(M_1/\pi)\mathrm{d}A_{1\perp}=(M_1/\pi)\mathrm{d}A_1\cos(\beta_1)$, $\mathrm{d}E_2=\mathrm{d}I_1\cos(\beta_2)/d_{12}^2=(M_1\mathrm{d}A_1)\cos(\beta_1)\cos(\beta_2)/d_{12}^2$; again, when $\mathrm{d}E_2(\theta)$ is plotted for given data (R,H), a bell-shape irradiance distribution is obtained, with a maximum at the closest point, $\mathrm{d}E_2(0)=(M_1\mathrm{d}A_1/\pi)/H^2$, falling to zero at the tangential point more quickly than in the case of the point source.

If the emitting patch is not parallel to the sphere (Fig. 14), but tilted an angle β, two cases must be considered, depending on the relative position of the sphere and the plane passing by the patch, what is delimited by the semi-angle subtended by the tangent to the sphere from the patch centre, $\beta_t=\arcsin(R/(R+H))$: if $\beta<\pi/2-\beta_t$, the whole projected sphere is seen by the patch; if $\beta>\pi/2+\beta_t$, no part of the projected sphere is seen by the patch; and if $\pi/2-\beta_t<\beta<\pi/2+\beta_t$, only a part of the projected sphere is seen by the patch. Let us solve the first case, i.e. $0<\beta<\pi/2-\arcsin(R/(R+H))$. The irradiation on a small spherical patch centred at the point (x,y,z), with $z=\sqrt{R^2-x^2-y^2}$, is again $\mathrm{d}E_2=\mathrm{d}I_1\cos(\beta_2)/d_{12}^2=(M_1\mathrm{d}A_1)\cos(\beta_1)\cos(\beta_2)/d_{12}^2$, but now the parameters are: $d_{12}=\sqrt{x^2+y^2+(R+H-z)^2}$, $\cos(\beta_1)=(d_{12}^2+d_0^2-d_1^2)/(2d_{12}d_0)$, $d_0=(R+H)/\cos(\beta)$, $d_1=\sqrt{\left(x-\left(H+R\right)\tan\left(\beta\right)\right)^2+y^2+z^2}$, and $\beta_2=\mathrm{sgn}(x)\arcsin\left(\sqrt{x^2+y^2}\,/R\right)+\beta-\beta_1$; to better grasp this cumbersome (although explicit) solution, Fig. 14 presents a contour plot of the irradiance distribution in the sphere, for the limit case where $\beta=\pi/2-\beta_t$ when $H=R$.

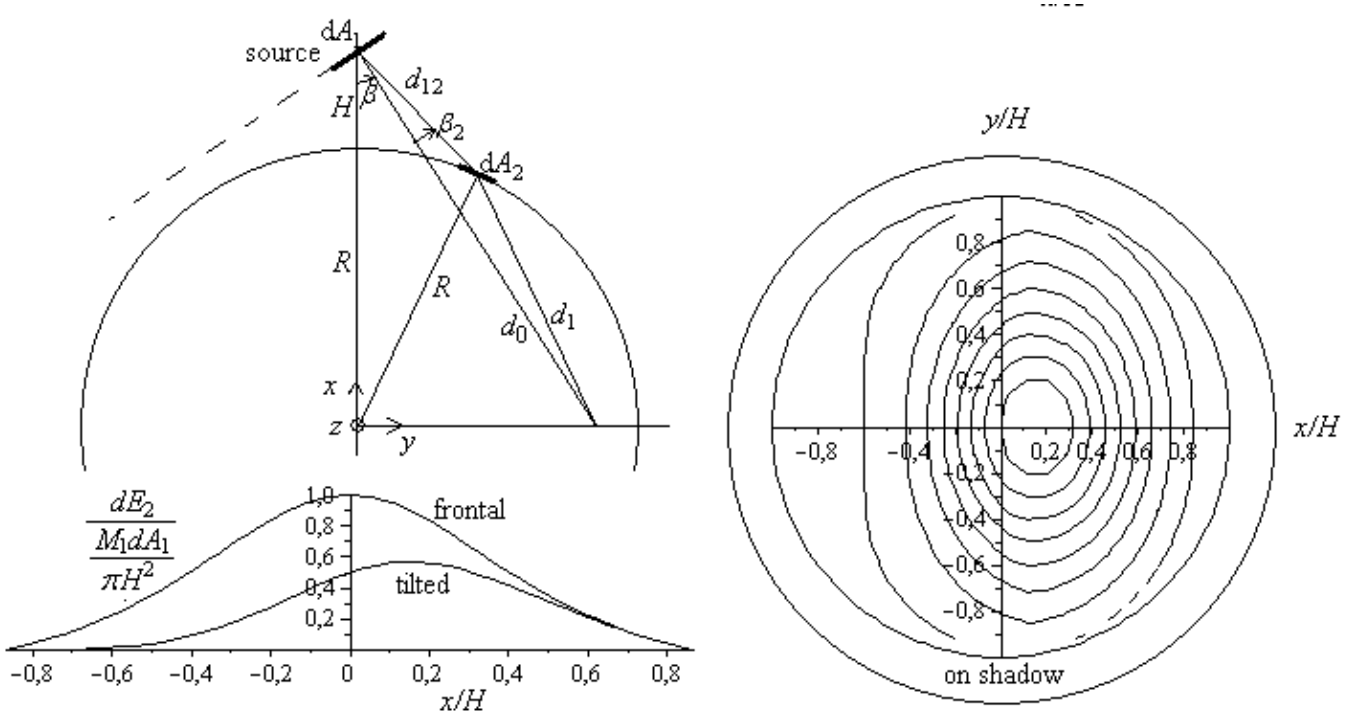

Fig. 14. Geometric sketch, and irradiance distribution, dE_2, on a sphere of radius R, due to a small radiation patch dA_1 of emittance M_1 at a distance H; a contour plot for the latter is plotted for the limit case $\beta=\pi/2-\beta_t$, with $\beta_t=\arcsin(R/(R+H))$ (i.e. 60º tilted patch, with 30º tangent angle, for $H=R$), and a profile of the irradiances at the central line $y=0$ for both $\beta=1.05$ rad (60º tilted patch) and .$\beta=0$ (parallel patch).

Radiation from a sphere to a small patch

Consider the radiation from a large spherical surface of radius R to a small tilted patch of area dA_1, separated a distance H from the surface. Again, we only consider the case of an isothermal sphere (i.e. uniform emittance), and proceed directly to compute the power received by the patch dA_1. Again, two cases must be considered, delimited by the semi-angle subtended by the tangent to the sphere from the patch centre, $\beta_t=\arcsin(R/(R+H))$:

- Case A, the plane containing the patch dA_1 does not cut the sphere, i.e. the patch tilting, β, is small, with $\beta<\pi/2-\beta_t$. In this case, the view factor can be found geometrically by the projections method (it is the area of the projection on the patch-plane of the projection of the radiating sphere on the unit hemisphere centred at dA_1, and divided by π):

$$F_{12}=\int\frac{\cos(\beta_1)\cos(\beta_2)}{\pi r^2}\mathrm{d}A_2=\frac{\cos(\beta)}{(1+h)^2} \qquad (43)$$

- Case B, the plane containing the patch dA_1 cuts the sphere, i.e. the patch tilting, β, is large, with $\pi/2-\beta_t<\beta<\pi/2+\beta_t$. In this case, the view factor is (Chun and Naragui, 1981):

$$F_{12}=\frac{\cos(\beta)}{\pi(1+h)^2}\left(\pi-\arccos(x)-xy\tan^2(\beta)\right)+\frac{1}{\pi}\arctan\left(\frac{y}{x}\cos(\beta)\right) \qquad (44)$$

with $x\equiv\sqrt{2h+h^2}\,/\tan(\beta)$ and $y\equiv\sqrt{1-x^2}$.

Radiation from a disc to a small patch

Consider the radiation from a disc of radius R to a small facing patch of area dA_2, axially located at a distance H (Fig. 15). Again, we only consider the case of an isothermal disc, i.e. uniform disc emittance, M_1 ($M_1=\sigma T^4$ if a blackbody). The power received by the patch dA_1 is $d\Phi_{12}=M_1A_1dF_{12}=M_1dA_2F_{21}=M_1dA_2R^2/(R^2+H^2)$, where the view factor from patch to disc, F_{21}, has been obtained from compilations.

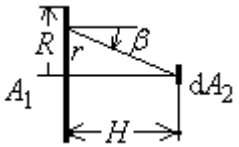

Fig. 15. Radiation from a disc of area $A_1=\pi R^2$ to a small frontal patch of area dA_2. Elementary area $dA_1=2\pi r dr$ tilted an angle β to the viewing direction.

Irradiance at the patch is $E_2=d\Phi_{12}/dA_2=M_1R^2/(R^2+H^2)=\pi L_1R^2/(R^2+H^2)=A_1L_1/(R^2+H^2)$, where disc radiance, L_1, has been introduced, because we want now to deduce it directly without recourse to view factor compilations. Consider a differential ring at a radial position r on the disc, of area $dA_1=2\pi r dr$. From the definition of radiance, $L_1\equiv d^2\Phi_{12}/(dA_1 d\Omega_{12}\cos\beta_1)$, where β_1 is the angle the direction $dA_1\rightarrow dA_2$ forms with the normal to dA_1, and $d\Omega_{12}$ the solid angle subtended, which is the projected area divided by the square of the distance, i.e. $d\Omega_{12}=dA_2\cos\beta_2/(r^2+H^2)$, what yields:

$$\left.\begin{aligned} d^2\Phi_{12} &= L_1 d\Omega_{12} dA_1 \cos\beta_1 = L_1\left(\frac{dA_2\cos\beta_2}{H^2+r^2}\right)(2\pi r dr)\cos\beta_1 \\ \rightarrow\quad d\Phi_{12} &= \int d^2\Phi_{12} = 2\pi L_1 dA_2 \int_{r=0}^{R}\frac{\cos^2\beta}{H^2+r^2}dr = \pi L_1 dA_2\frac{R^2}{H^2+R^2} \\ E_2 &= \frac{d\Phi_{12}}{dA_2} = \frac{\pi L_1 R^2}{H^2+R^2} = \frac{L_1 A_1}{H^2+R^2}\xrightarrow{H>>R} L_1\Omega_{12} \end{aligned}\right\} \qquad (45)$$

i.e., we have recovered the previous result, and we see that, if the disc source is far enough, like our Sun, the irradiance we get is simply the radiance times the solid angle subtended.

Summary of radiation laws

Laws of radiation propagation:

- Straight propagation. Radiation propagates in straigh line at the constant speed of light (under vacuum; if propagation is through media of refractive index n, then the speed is c/n and direction may change by refraction).
- Inverse square law of irradiance from a point source. Radiation from a finite source in non-absorbing media decays with the inverse of the distance square, due to energy conservation through the englobing spheres, i.e. $E=E_0(d_0/d)^2$.
- Cosine law of irradiance on an inclined plate from a parallel beam. For a given collimated radiation of normal irradiance E_0, irradiance upon a tilted surface is $E_\theta=E_0\cos\theta$, where is the azimuthal angle of incident radiation.
- Cosine cube law of irradiance at a horizontal plate from a point source: $E_{horiz}=E_{normal}\cos\theta=E_{max}\cos^3\theta=(I/H^2)\cos^3\theta$.

Laws of radiation emission:

- Cosine law for exitance. The power emitted by a blackbody patch (and by extension the power emiited and the power reflected by a Lambertian surface patch), decreases from the normal direction by Lambert's law, $M_\theta = M_0 \cos\theta$.
- Planck law of blackbody emission: $M_\lambda = A/\{\lambda^5[\exp(B/(\lambda T))-1]\}$, with $A = 0.374 \cdot 10^{-15}$ W·m^2 and $B = 0.0144$ m·K.
- Stefan-Boltzmann law of blackbody emission: $M = \sigma T^4$, with $\sigma = 5.67 \cdot 10^{-8}$ W/(m^2·K^4).
- Wien displacement law of blackbody emission: $\lambda_{M\max} = C/T$ with $C = 0.00290$ m·K. In terms of frequency, $\nu_{M\max} = C'T$ with $C' = 58.8 \cdot 10^9$ Hz/K.
- Kirchhoff's law. Detailed thermodynamic equilibrium at a given temperature T of radiation exchange at an opaque surface, implies that emissivity at a given wavelength λ in a given direction (ϕ,θ), must be equal to absorptance of radiation of the same wavelength coming from the same direction, $\varepsilon_{T,\lambda,\phi,\theta} = \alpha_{T,\lambda,\phi,\theta}$. With the grey surface model, $\varepsilon_{IR} = \alpha_{IR}$.

Laws of view factor algebra:

- Bounding. View factors are bounded to $0 \le F_{ij} \le 1$ by definition (the view factor F_{ij} is the fraction of energy exiting surface i, that impinges on surface j).
- Closeness. Summing up all view factors from a given surface in an enclosure, including the possible self-view factor for concave surfaces, $\sum_j F_{ij} = 1$, because the same amount of radiation emitted by a surface must be absorbed.
- Reciprocity. Noticing from the above equation that $dA_i dF_{ij} = dA_j dF_{ji} = (\cos\beta_i \cos\beta_j/(\pi r_{ij}^2))dA_i dA_j$, it is deduced that $A_i F_{ij} = A_j F_{ji}$.
- Distribution. When two target surfaces are considered at once, $F_{i,j+k} = F_{ij} + F_{ik}$, based on area additivity in the definition.
- Composition. Based on reciprocity and distribution, when two source areas are considered together, $F_{i+j,k} = \left(A_i F_{ik} + A_j F_{jk}\right) / \left(A_i + A_j\right)$.

Back to Spacecraft Thermal Control

Back to Heat transfer

Back to Thermodynamics